C.P. No. 1252

C.P. No. 1252

PROCUREMENT EXECUTIVE, MINISTRY OF DEFENCE

AERONAUTICAL RESEARCH COUNCIL

CURRENT PAPERS

A Suggestion for Improving Flap Effectiveness by Heat Addition

by

J. Martin

Aerodynamics Dept., R.A.E., Farnborough

LONDON: HER MAJESTY'S STATIONERY OFFICE

1973

PRICE 85p NET

UDC 533.694.65 : 533.694.511 : 533.6.048.2 : 533.694.7

CP No.1252*
January 1972

A SUGGESTION FOR IMPROVING FLAP EFFECTIVENESS BY HEAT ADDITION

by

J. Martin**

SUMMARY

The effect of a particular type of heat addition on the flow around a two-dimensional, flapped aerofoil section, at low Mach number, is investigated using a transformation which enables the compressible flow with heat addition to be deduced approximately from a certain incompressible flow with fluid addition. The incompressible flow may be determined by the technique of conformal mapping. It is concluded that heat addition in a suitable distribution can so reduce the adverse pressure gradient on the upper surface of the flap that greater flap angles than are normally possible can be employed without separation of the boundary layer (according to a simple separation criterion). The result is an increase in lift. The effect is illustrated for a flapped aerofoil section of convenient mathematical form.

---

* Replaces RAE Technical Report 72002 - ARC 33876

**Vacation Student, Aerodynamics Department, RAE, during the summer of 1970. Now at Department of Mathematics, University of Manchester.

CONTENTS

1 INTRODUCTION

The effect of heat addition on low speed flow of an inviscid fluid was discussed by Broadbent[1], who demonstrated that in a flow region where

$$p \frac{D}{Dt} (1/\rho) \gg \frac{1}{\rho} \frac{Dp}{Dt}$$

that is to say, where pressure variations are small compared with variations in specific volume, an approximate solution of the relevant flow equations can be obtained by a simple transformation of the solution of a certain incompressible flow problem. This problem retains the geometry of the original but replaces heat sources by fluid sources. Under the transformation, pressure distributions are unchanged. In the present Report, this property is used to discuss the effect of heat addition on twodimensional flow past a lifting aerofoil section, with particular reference to the modification of pressure gradients near trailing-edge flaps.

The possibility was suggested by Broadbent[2] that a suitable heat source distribution, placed in the neighbourhood of the upper surface of a trailing-edge flap might reduce the adverse pressure gradient there to such an extent that large flap deflection angles could be achieved without the onset of boundary layer separation (a conventional flap with no slots or blowing is assumed). A first investigation[2] of the effect of heat addition on adverse pressure gradients was made using a simple Joukowski aerofoil, with sufficiently encouraging results to prompt an examination of the effect on a flow past an aerofoil in a configuration of high lift, that is with a trailing-edge flap deflected. The essential qualitative features should be exhibited for any reasonably realistic aerofoil with a flap. In the sequel, the twodimensional case is considered, and a family of profiles used which is convenient for the application of complex variable methods.

When a flap is deflected, in low speed flow, its primary effect is to increase the circulation around the aerofoil and so increase lift. The undesirable secondary effect is to increase the adverse pressure gradient along the upper surface of the flap. As the flap deflection is increased, there will thus come a point when the flow will separate, resulting in considerable loss of lift. In this Report, the complicated problem of boundary layer separation will be simplified by the assumption that separation depends only on the magnitude of the local adverse pressure gradient. With some standard upstream

flow speed and angle of attack, one may define a critical flap angle $\alpha^{o}\pi$ rad, at which separation occurs. This angle, in turn, defines a maximum adverse pressure gradient G^{o} under which an attached boundary layer can subsist in the region above the flap, and a maximum lift coefficient C_L^{o} which can be achieved by this flap mechanism.

Can this situation be improved by heat addition near the flap? If, by adding heat, the adverse pressure gradient along the upper surface of the flap can be reduced then, according to the above criterion, it may be possible to operate the flap at angles $\alpha\pi > \alpha^{o}\pi$ without separation (i.e. with a maximum adverse pressure gradient on the flap of $G \leqslant G^{o}$) and with an increase in lift $(C_L > C_L^{o})$.

According to the first paragraph, this problem can be transformed into one involving fluid addition in incompressible flow. Subsequent analysis applies only to the inviscid, external flow field, the boundary layer being assumed to remain attached and of negligible thickness. When a solution of the incompressible, inviscid flow equations has been found, a decision may be made retrospectively whether a boundary layer on the flap could have remained attached under the conditions of pressure gradient predicted.

Whilst adverse pressure gradients can certainly be reduced by heat addition, and so larger flap angles achieved without separation, it is not obvious that lifting properties will be improved. There is a secondary effect, namely the reduction of total circulation (assuming the source is added above the aerofoil). It is part of the investigation to compare this loss of circulation (and hence lift) with the increase which can be gained from the use of greater flap angles.

In section 2, the analogy between incompressible flow with fluid addition and compressible flow at low Mach number with heat addition is examined and the approximations discussed. The central problem of the Report is treated in section 3. As far as possible, progress has been made analytically using complex function theory and conformal mapping. It is therefore necessary to find a reasonably realistic flapped aerofoil section which is the image, under a conformal mapping, of one of the geometric shapes for which the flow equations can be solved by elementary methods (e.g. a circle). This is done in Appendix A. The standard expressions for velocity, pressure etc. are set up in Appendix B, and a numerical method is considered in Appendix C. Numerical results are discussed in section 4.

2 THE INCOMPRESSIBLE FLOW - COMPRESSIBLE FLOW ANALOGY

2.1 A statement of the analogy

The analogy between compressible flow at low Mach number with heat addition and incompressible flow with fluid addition was set up by Broadbent[1] and a discussion sufficient for the present purpose, using simpler mathematical ideas was given by Edwards[3]. This discussion is summarised here. More precisely, the analogy is between:

(a) an incompressible flow with a fluid source distribution (and possibly also a system of body forces) in a finite region;

and (b) a compressible flow in which a heat source distribution and an additional system of body forces replace the fluid source distribution of the incompressible analogue.

Suppose the flow (a) is fully defined so that in particular, the pattern of streamlines, the pressure field, and the fluid source distribution (and if appropriate, the body force distribution) are known. An attempt is made to determine a compressible flow which has precisely the same streamlines and pressure field, but in which the fluid source distribution is replaced by a heat source distribution and an additional body force distribution (the heat and body force may be thought of in combination simply as an energy source distribution). This process may be shown possible, giving rise, however, to a 'compressible flow' in which there may be large variations of density due to variations in temperature caused by the heat addition, but variations of pressure are too small to cause changes of temperature and density. This fact limits the 'compressible flow' to Mach numbers at which normal compressibility effects are negligible. The identity of streamlines and pressure in the two flows, implies the identity of momentum flux also.

The analogy may be used to determine compressible flows at low Mach number with energy addition, by first solving an incompressible flow problem with fluid addition. The approximation so introduced is precisely that which is always associated with the use of incompressible flow calculations for low Mach number flows. The 'heat flap' problem subsequently discussed, concerns a high lift device used at landing and take-off when speeds are low, so that the use of the analogy would appear justified. The following discussion is expressed in the geometry of flow past an aerofoil as will subsequently be required, although the analogy is of far more general application.

2 2 Justification of the analogy

A full justification of the analogy would require a proof that a compressible flow with energy addition exists which has streamlines and pressure distribution identical with those of the incompressible flow. This can be done following the method of Broadbent[1], but here, existence is assumed and a suitable energy source distribution obtained by identifying a limited set of properties of the two flows.

Fig.1 depicts the flow about a twodimensional aerofoil section. Only two streamlines are shown, and they are supposed to include the streamtube S. Station 0 is supposed to be far upstream, and station 1 far downstream. Between stations 2 and 3 and in the tube S, is a region R which is supposed to contain the source and body force distributions. In order to present a simple physical theory, it is supposed that the streamtube S is sufficiently thin that the flow within may be assumed uniform across any section. In the incompressible flow the region R contains a fluid source distribution so that the streamtube is thicker far downstream of R than it is upstream. An identical thickening of the streamtube in the compressible case can be achieved by heat addition (which raises the temperature and reduces the density) although to satisfy the requirement that the momentum flux should be the same in both flows, it can be shown that mechanical energy (or equivalently, momentum) must also be added, by means of a body force distribution.

Suppose A = thickness of tube S
m = total strength of fluid source distribution in the incompressible flow
Q = total strength of energy source distribution (heat and mechanical energy) in compressible flow
p = pressure
U = flow speed
γ = ratio of specific heats of stream fluid
ρ = density.

The suffices 0, 1 are used in both flows to denote conditions at stations 0, 1. The extra suffices i, c are used to distinguish incompressible flow and compressible flow variables.

In the incompressible flow, conditions far upstream and far downstream are the same, and density is the same everywhere, hence:

$$p_{1i} = p_0 \qquad U_{1i} = U_0 \qquad \rho_{1i} = \rho_0 = \rho \ .$$

At all corresponding points in the two flows, the pressures are equal, hence, in particular,

$$p_{1c}' = p_{1i} \ .$$

A consequence of the correspondence between the pressure fields is that the Mach number of the compressible flow must be approximately the same as that of the incompressible flow (i.e. very small). Variations of density in the compressible flow are therefore only associated with variations in temperature and do not arise from variations in pressure. The variations in temperature are due to energy introduced into the compressible flow through the energy source distribution.

Since the streamline patterns of the two flows are identical, the stream-tube thickness A is the same, for each flow, at every station, and in particular,

$$A_{1c} = A_{1i} = A_1 \qquad \text{(say)} \ .$$

The equations of conservation of mass for the two flows read:

$$\rho_0 U_0 A_0 = \rho_0 U_0 A_1 - \rho_0 m \qquad \text{(incompressible)}$$
$$\rho_0 U_0 A_0 = \rho_{1c} U_{1c} A_1 \qquad \text{(compressible)} \ .$$

The equation of conservation of energy in the compressible flow reads:

$$\rho_0 U_0 A_0 \left\{ \frac{\gamma}{\gamma - 1} \frac{p_0}{\rho_0} + \tfrac{1}{2} U_0^2 \right\} = \rho_{1c} U_{1c} A_1 \left\{ \frac{\gamma}{\gamma - 1} \frac{p_{1c}}{\rho_{1c}} + \tfrac{1}{2} U_{1c}^2 \right\} - Q \ .$$

The last three equations express conservation of quantities along the tube S. This is clearly reasonable in the case of mass, and is justified for energy on neglecting diffusion.

The momentum flux at all corresponding stations is to be equal in the two flows, and in particular, at the downstream station:

$$\rho_0 U_0^2 A_1 = \rho_{1c} U_{1c}^2 A_1 \quad .$$

All the downstream variables may be eliminated between the forgoing equations and there follows

$$Q = \rho_0 m \left\{ \frac{\gamma}{\gamma - 1} \frac{p_0}{\rho_0} + \tfrac{1}{2} U_0^2 \right\} \left(2 + \frac{m}{U_0 A_0} \right) \quad ,$$

an expression which relates the fluid source strength m to the energy source strength Q and involves only known or controllable quantities. In general, the energy Q will be mainly heat energy. In fact, it can be shown that if the local flow speed in the source region is U, the pressure p, and the density ρ, the energy added as heat is

$$Q_H = \rho_0 m \frac{\gamma}{\gamma - 1} \frac{p}{\rho} \left(2 + \frac{m}{U_0 A_0} \right)$$

and the energy added as mechanical energy is

$$Q_K = \rho_0 m \tfrac{1}{2} U^2 \left(2 + \frac{m}{U_0 A_0} \right) \quad .$$

The mechanical energy component divided by the heat component is thus equal to

$$(\tfrac{1}{2} U^2) \Big/ \left(\frac{\gamma}{\gamma - 1} \frac{p}{\rho} \right) = \tfrac{1}{2} (\gamma - 1) M^2$$

where M is the Mach number. Only flow at low Mach number is under consideration so that this ratio is small. Hence the rate of input of heat Q_H may be accepted as a good approximation to the total energy input Q. Similarly, it is clear that:

$$Q = \frac{\gamma}{\gamma - 1} p_0 m \left(2 + \frac{m}{U_0 A_0} \right) [1 + \tfrac{1}{2} (\gamma - 1) M_0^2]$$

(M_0 = upstream Mach number). The leading term of this (neglecting M_0) involves only m and upstream variables, and will be taken, in subsequent applications, as the approximation for both Q and Q_H:

$$Q \simeq Q_H \simeq \frac{\gamma}{\gamma - 1} p_0 m \left(2 + \frac{m}{U_0 A_0} \right) \quad .$$

3 FLOW ABOUT A FLAPPED AEROFOIL SECTION

3.1 A family of flapped aerofoil sections

It is assumed that the 'heat flap' effect under discussion may be exhibited by any reasonably realistic aerofoil with variable flap deflection. The analogy discussed in the previous section leads to a twodimensional, incompressible, irrotational* flow problem (for which solution by complex variable techniques is standard) and so it is convenient to employ profiles which can be mapped by a simple conformal transformation on to one of the geometrical shapes for which the flow equations can be solved by an elementary technique (e.g. a circle). It is necessary, then, to determine a family of profiles in this class which may reasonably be thought of as one aerofoil under various conditions of flap deflection. This is done in Appendix A. Each profile is defined by the parameters:

L = chord length of wing from leading edge to the knee of the flap
δ = ratio flap chord length to L
α ($\alpha\pi$ rad = flap deflection angle)
ε = 'thickness parameter' - see Appendix A

and the profile so determined is denoted $P(L,\delta,\alpha,\varepsilon)$. Variation of the parameter α is supposed to provide the required variation of flap deflection.

The profile is obtained from the circle $C(\varepsilon)$ in the complex ζ-plane, having centre the point $-\varepsilon$, and radius $1 + \varepsilon$ ($C(\varepsilon)$ thus passes through the point $\zeta = 1$). The region exterior to $C(\varepsilon)$ is denoted $D(\varepsilon)$, and is mapped onto the region exterior to $P(L,\delta,\alpha,\varepsilon)$, regarded as lying in a complex z-plane, by the mapping $F_{L,\delta,\alpha}$. For brevity, the arguments of P, C and D, and suffices of F will often be dropped. The details of F are given in Appendix A and Figs.14 and 15. The properties pertinent here are:

(a) F is conformal throughout D except at the point $\zeta = 1$ ($\varepsilon > 0$)
(b) $F(1) = L \exp(-i\alpha\pi)$ (trailing edge)
(c) $F'(\zeta) \to 0$ as $\zeta \to 1$
(d) $F(\zeta) \to \infty$ as $\zeta \to \infty$
(e) $F'(\zeta) \to$ a constant, Λ as $\zeta \to \infty$.

The profile is located in the z-plane with the knee of the flap at the origin and the main wing profile along the negative real axis.

---

* The incompressible flow is irrotational, but rotationality is introduced in the compressible flow by the transformation.

3.2 The incompressible flow problem

With a conformal mapping as quoted above, any incompressible, irrotational flow in the profile plane is simply related to an incompressible, irrotational flow in the circle plane. The precise relationship is given in Appendix B, together with a direct determination of the circle plane flow. The profile plane flow is uniquely determined by the following requirements:

(a) The zero normal velocity condition on the aerofoil.

(b) The condition at infinity - the velocity must approach that of the free stream.

(c) Since the flow region is doubly connected, a condition fixing the circulation around the aerofoil - this is provided by Joukowski's hypothesis.

(d) The existence of certain flow singularities - sources, doublets, etc., or distributions of source. In this Report, only sources and source distributions are introduced.

On the basis of Appendix B, it is thus possible to determine all characteristics of the flow around any quoted profile P for given far-flow conditions, and fluid source distributions. In particular, the following may be calculated:

(a) Lift coefficient $C_L = \dfrac{\text{total lift force}}{\frac{1}{2}\rho_0 U_0^2 c}$.

(b) Pressure coefficient $C_p = \dfrac{p - p_0}{\frac{1}{2}\rho_0 U_0^2} = 1 - \left(\dfrac{U}{U_0}\right)^2$ (by Bernoulli's equation).

Here, c = total chord of aerofoil $\simeq L(1 + \delta)$ for α and ε small

U = local flow speed $\quad U_0 = U(\infty)$

p = local pressure $\quad p_0 = p(\infty)$

ρ_0 = undisturbed density = constant density of incompressible flow.

The lift force mentioned here may be calculated as $\rho_0 U_0 \kappa$ (κ = circulation). There is really another term representing the force directly on the source distribution, but as this is of the order of magnitude of the total source strength (which is small in all applications) it is negligible. Similarly, the drag is modified by an extra small term. The coefficients C_L and C_p may be applied directly to the analogous compressible flow with heat addition, as discussed in section 1.

3.3 Plan for numerical investigation

In the next section, the following cases are examined numerically using the results just set up:

(a) A profile $P(L,\delta,\alpha^o,\varepsilon)$ under certain standard conditions at infinity, with a maximum adverse pressure gradient on the flap of G^o and lift coefficient C_L^o is taken as a datum condition, which for realism would be chosen to represent the 'critical' situation where flow over the flap is on the point of separation (possibly determined by experiment).

This case will be used to define:

(i) A lift coefficient which is the theoretical maximum obtainable by the flap mechanism under flow conditions with no recirculation.

(ii) A maximum adverse pressure gradient on the flap which can be withstood by the boundary layer (it is assumed that the maximum tolerable adverse pressure gradient varies little over the length of the flap).

(b) Another profile $P(L,\delta,\alpha,\varepsilon)$ with $\alpha > \alpha^o$ under the same conditions at infinity. In the absence of sources, this profile leads to a flow with a maximum adverse pressure gradient on the flap larger than G^o so that separation is predicted by the above criterion, recirculation occurs and the solution is invalidated. However, the solution will imply a lift coefficient $C_L^1 > C_L^o$. If now a heat source distribution is devised which modifies the flow in such a way that the new maximum adverse pressure gradient on the flap is $G \leqslant G^o$ and the lift coefficient is C_L $(C_L^o < C_L < C_L^1)$, it will have been shown explicitly that greater lift can be achieved using heat as a 'catalyst' to keep the boundary layer attached. It remains

(i) to determine suitable heat distributions

(ii) to characterise the results of (b) in some way which will enable judgments of efficiency of the 'heat flap' to be made (compared with other high lift devices).

3.4 Determination of suitable source distributions

The determination of suitable fluid source (or equivalently heat) distributions is governed by three considerations:

(a) the requirement to ensure $G \leq G^o$

(b) the requirement $C_L > C_L^o$

(c) the need to add heat over a streamtube sufficiently thick to ensure that the factor $2 + m/U_0 A_0$ in the expression for Q the required heat addition (section 2.2) is not too large.

It is convenient to work initially in the circle plane (ζ-plane) and to describe the source distribution by polar coordinates (r,θ) defined by $\zeta = r \exp(i\theta) - \varepsilon$ (that is with respect to the centre of the circle $C(\varepsilon)$ - Fig.2). The corresponding profile plane distribution can be obtained by the transformation F and it is convenient to use coordinates (h,s) shown in Fig.2; s is the distance around the upper surface of the profile from the trailing edge to the foot of the profile normal passing through the point in question; h is the distance from the profile along the profile normal. The system is only well defined in the unshaded region of Fig.2 but all points of interest are in this region.

Consideration (a) essentially governs the distribution in the s-direction and is not very sensitive to the precise h-distribution. Consideration (c) affects the h-distribution only. Consideration (b) restricts the total source strength but is not strongly related to the spatial distribution.

For the purpose of calculation it is very convenient to regard the fluid as being added in point sources, but this is inconsistent with requirement (c) since in this case, $A_0 = 0$. Nevertheless, it is reasonable to suppose that the 'heat flap' effect is not strongly dependent on the h-distribution and so a calculation using point sources would differ little from a calculation using the same total source strength in a distribution smoothed out along the profile and over a band of non-zero thickness. This assumes that the point source distribution is located at a sufficient distance from the profile to ensure that its discrete nature does not cause violent fluctuations in the pressure gradient on the profile. In the sequel point source distributions are used to approximate continuous distributions. One continuous distribution is considered directly.

The s-distribution is governed by the requirement to reduce G to a value no greater than G^o. Suppose an existing flow pattern arising from the free stream and some source distribution is modified by the addition of a single new source (or concentrated source region) near the point z^*. The situation of interest occurs when:

(a) Both modified and unmodified flows have no stagnation points along the upper surface of the profile. In other words the sources are not too strong.

(b) The new source is added somewhere in the region above the upper surface of the flap.

The corresponding situation in the circle plane is shown in Fig.3. It is evident that the effect of superimposing the additional velocity distribution associated with the new source on the existing distribution, is to reduce the velocity gradient close to $\zeta^* = F^{-1}(z^*)$. A similar effect occurs in the profile plane. Thus close to z^* the adverse pressure gradient is also reduced although it is likely to have increased elsewhere. This suggests the possibility of adding heat in a suitable distribution to reduce the adverse pressure gradient where it is most serious at the expense of increasing it where it is less significant.

In the subsequent numerical work, the value of r at which point sources are added is arbitrarily selected and then suitable θ-distributions are obtained either by trial and error or by a systematic method given in Appendix C. Likewise, for the continuous distribution, the r-dependence is fixed by choosing the distribution independent of r over a range $1 + \varepsilon < a \leqslant r \leqslant b$, and zero for other values of r. The θ-distribution is obtained by trial and error.

3.5 The treatment of point source distributions

When a point source distribution is considered, it is necessary to assign to it a non-zero value of A_0. The justification for this is mentioned in the previous section. The actual value of A_0 selected is a matter of choice, but clearly the smaller its value, the more reasonable is the supposed relationship between the point source case and its continuous equivalent (and the more reasonable is the discussion in section 1). On the other hand the larger the value of A_0 the smaller is the factor $(2 + m/U_0A_0)$ in the heat consumption Q and hence the more efficient will the heat flap apparently be. Suitable streamtube thicknesses will also be affected by considerations of temperature rise and fuel to air ratio which might lead to combustion. It is evident that only the order of magnitude of Q will come convincingly from this sort of calculation, and so any reasonable value of A_0 will suffice. In all the point source distributions subsequently considered, the sources lie at a mean

height h^*L (with an error of no more than 10%) and so it would appear reasonable to select a streamtube of upstream thickness $A_0 = 0.2h^*L$ which extends equal distances above and below the mean line of sources. The tube thickness in the neighbourhood of the sources may then be shown to be of the same order of magnitude as the variation in height and the tube lies strictly outside the profile. The crucial factor $2 + m/U_0A_0$ is not strongly dependent on the choice of 0.2. Any value giving rise to $A_0 \gtrsim m/U_0$ is suitable. A typical value for m/U_0 subsequently obtained is 0.01 and h^* is 0.03 so that if $A = \phi h^*L$, any value of $\phi \gtrsim 0.1$ will not alter the final order of magnitude.

3.6 Parameters for the heat distributions

The two significant features of the system modified by increasing flap deflection, and adding heat are the extra lift obtained and the heat added. The former is clearly expressed by the increment in lift coefficient $C_{LQ} = C_L - C_L^o$. The heat addition may be conveniently expressed as a specific fuel consumption parameter C_F defined as:

$$\frac{\text{weight of fuel consumed by the 'heat flap' per unit time}}{\text{additional lift obtained.}}$$

It is necessary to introduce a suppose calorific value H for the fuel (units of energy per unit weight of fuel).

Suppose a particular heat source distribution involves a total heat addition rate Q per unit span

$$Q = \frac{\gamma}{\gamma - 1} p_0 m \left(2 + \frac{m}{U_0 A_0}\right) .$$

If U_0 and L are taken as velocity and length scales (L is the chord length of the profile from leading edge to flap knee - the total chord c is approximately equal to $L(1+\delta)$), it is clear that $m \propto U_0 L$. The rate of fuel consumption is Q/H and the additional lift developed is $\frac{1}{2}\rho_0 U_0^2 c C_{LQ}$, thus:

$$C_F = \frac{2Q}{\rho_0 U_0^2 c C_{LQ} H} = \frac{\gamma p_0}{\rho_0 H U_0} \left[\frac{2m(2 + m/U_0A_0)}{(\gamma - 1)U_0 c C_{LQ}}\right]$$

in which the square brackets contain a dimensionless quantity independent of velocity and length scales. C_F has dimensions 1/time, and U_0C_F is independent of velocity and length scales. If a total operating time t is assumed per

flight, the quantity tC_F measures the total extra fuel load divided by the extra lift (it is still inversely proportional to U_0). If, for a realistic value of U_0 this is small, whilst C_{LQ} is positive, the effectiveness of the 'heat flap' would have been shown, as far as is possible by the present analysis. Comparison can be made directly with specific fuel consumptions for other high lift devices (e.g. blowing flaps or lift engines).

In numerical work, SI units are used and a calorific value of 4.4×10^6 J/N is assumed for H. The operating time is taken as t = 200 s. Values of U_0C_F, U_0tC_F, and tC_F are tabulated, the latter with U_0 = 60 m/s.

4 RESULTS AND DISCUSSION

4.1 Notation and layout

All the symbols in this section are defined in section 3. Results for each solution are displayed in a combination of graph and table. Pressure distribution curves have $-C_p$ plotted against s over a range beginning at the trailing edge and running along the upper surface to well past the knee of the flap. Where a pressure distribution includes the effect of sources, the corresponding distribution before sources were added is shown for comparison. Point sources are depicted on graphs by a dot at the appropriate value of s, the information h, r, θ, m being given in a table.

4.2 The datum condition

The datum condition is taken to be the profile P(1.0,0.25,0.05,0.1) with $U_0 = 1$ and angle of attack 0.05π rad ($\simeq 9^\circ$). The values of the various parameters of the profile are thus:

$L = 1$
$\delta = 0.25$
$\alpha^\circ = 0.05$ (flap deflection angle, also about 9°)
$\varepsilon = 0.1$.

The aim of the calculation is to determine initially C_L° and subsequently consider C_{LQ} and U_0C_F for various source distributions. All these quantities are independent of U_0 and L which one is thus at liberty to take as unity. Additionally, C_{LQ} is dimensionless whilst U_0C_F has the dimensions of length and will be expressed in whatever units of length are used in the constant quantities, H, p_0, ρ_0. The profile is depicted in Fig.17a, and the pressure distribution for no additional sources is shown in Fig.4. The adverse pressure

gradient $G(s)$ is the positive slope of this graph. Very close to the trailing edge, G is large ($G \sim 9$ for $s \sim 0.002$), it then falls to values of order 3, then rises to a local maximum of 6.16 at $s = 0.2509$, which is very close to the flap knee. Later G becomes negative, and is only large and positive again at and beyond $s \sim 0.6$ which is outside the present region of interest. One must discount the large G-value at $s \sim 0.002$, since such values inevitably occur on any non-symmetrical aerofoil. This is essentially admitting that a separation does occur very close to the trailing edge and trusting that the inviscid solution outside the boundary layer is not appreciably affected other than in a thin wake extending back from the trailing edge. This kind of problem is discussed by Smith[4] although it is not yet possible to give a final conclusion on the importance of the trailing edge separation in distorting the flow further upstream. The value to be taken as G^o, the maximum tolerable adverse pressure gradient on the flap, is 6.16 which occurs close to the flap hinge. The lift coefficient in the datum condition is $C_L^o = 1.67$.

4.3 The first comparison case

Consider next, the profile P(1.0,0.25,0.075,0.1), with the same upstream velocity $U_0 = 1$ and angle of attack = 0.05π rad. The only change is that the deflection angle of the flap becomes 0.075π rad ($\simeq 13.5^o$). The profile is depicted in Fig.17b. In the absence of sources, the maximum adverse pressure gradient on the flap is 10.34 (so that separation is predicted by the criterion previously set up) and the lift coefficient is $C_L^1 = 1.96$. A selection of source distributions which will reduce the maximum adverse pressure gradient on the flap to a value no greater than G^o (= 6.16) is presented in Figs.5-9. Some of the distributions are obtained by trial and error, others by the systematic method (quoting a maximum tolerable adverse pressure gradient of 6.16 in one case and 5 and 3 respectively in the other two cases, to show the possibilities of the method). The relative efficiencies may be judged from the following table:

Figure No. (te) trial and error (s) systematic	Max. adverse pressure gradient on flap	C_{LQ}	$U_0 C_F$ (m/s^2)	$U_0 tC_F$ (m/s)	tC_F (U_0 = 60 m/s)
5(te)	5.65	0.25	0.014	2.8	0.046
6(te)	5.56	0.21	0.047	9.4	0.156
7(s)	6.16	0.26	0.008	1.6	0.027
8(s)	5.00	0.245	0.014	2.9	0.048
9(s)	3.00	0.16	0.104	20.8	0.346

In calculating these figures, the following values have been used:

$$\gamma = 1.4$$
$$H = 4.4 \times 10^6 \text{ J/N}$$
$$t = 200 \text{ s}$$
$$p_0 = 10 \text{ N/m}^2$$
$$\rho_0 = 1.2 \text{ kg/m}^3$$
$$A_0 = 0.2h*L$$

The most efficient of these solutions is that described by Fig.7. For this solution, a 15.5% increase in lift is achieved by a heat addition described by a specific fuel consumption at 60 m/s of 0.48 lb wt fuel per hour per lb of lift force. This figure is quite comparable with the specific fuel consumptions for e.g. fan lift engines.

4.4 The second comparison case

Consider the profile P(1.0,0.25,0.1,0.1), with the same upstream velocity $U_0 = 1$ and angle of attack = 0.05π rad. The only change is that the deflection angle of the flap has been increased again to 0.1π rad ($\simeq 18^\circ$). The profile is depicted in Fig.17c. In the absence of sources, the maximum adverse pressure gradient on the flap is 15.58 (so separation is predicted) and the lift coefficient $C_L^1 = 2.25$. Three source distributions which will each reduce the maximum adverse pressure gradient on the flap to a value no greater than G° (= 6.16) are presented in Figs.10-12. The efficiencies may be judged from the following table:

Figure No. (te) trial and error (s) systematic	Max. adverse pressure gradient on flap	C_{LQ}	$U_0 C_F$ (m/s^2)	$U_0 tC_F$ (m/s)	tC_F (U_0 = 60 m/s)
10(te)	6.15	0.47	0.046	9.3	0.155
11(s)	6.16	0.50	0.019	3.8	0.063
12(s)	5.00	0.47	0.032	6.3	0.105

Here the most efficient solution is that described in Fig.11. A 30% increase in lift is achieved by a heat addition described by a specific fuel consumption at 60 m/s of 1.14 lb wt fuel per hour per lb of lift force.

4.5 Continuous source distribution

Consider the profile used in the first comparison case (section 4.3) with an equivalent fluid source distribution defined in the circle plane as $\mu(\zeta^*)$ where:

(a) $\mu \neq 0$ only in a region R(circle) consisting of points $\zeta^* = (r,\theta)$ with $1.15 < r < 1.25$ and $33^\circ < \theta < 52.5^\circ$.

(b) In R(circle), μ is a function of θ only and

$$\mu(\theta) = 0.0044(\theta - 33)^2 \qquad 33^\circ < \theta < 45^\circ$$

$$\mu(\theta) = 1.3 - 0.025(\theta - 50)^2 \qquad 45^\circ < \theta < 52.5^\circ$$

(θ measured in degrees in the calculation of μ). This distribution is shown diagrammatically in Fig.13. The corresponding source distribution in the profile plane occupies an approximate region R(profile) consisting of points (h,s) with $0.12 < s < 0.26$ and $0.02 < h < 0.05$, which extends in a narrow band above the aerofoil from a point about half way along the flap to just past the flap knee (Fig.13). Data for this source distribution is also shown in Fig.13 and in particular

Max. adverse pressure gradient on flap = 4.19

C_{LQ} = 0.25

$U_0 C_F$ = 0.032 m/s^2

$U_0 tC_F$ = 6.4 m/s

tC_F (U_0 = 60 m/s) = 0.11

Here a 12.5% increase in lift is obtained by heat addition with a specific fuel consumption at 60 m/s of 1.92 lb wt fuel per hour per lb of lift force.

4.6 Energy addition in practice

It was noted in section 2.2 that the method of analysis used implies that the heat addition is accompanied by a definite amount of momentum addition. At low Mach numbers the total energy supplied is only very slightly greater than the part supplied as heat, but although the supply of heat alone may be relatively straightforward the supply of momentum as well may be more difficult, since some form of propulsive system would be needed.

It is therefore of interest to speculate on the possible effect of adding heat alone. The streamlines would then be affected and in view of the momentum deficit one would expect the streamtubes to get locally fatter. This may slightly change the optimum position of the heat source, but qualitatively the general effect should be similar to that found in the analysis, and may even be rather more powerful. No doubt this point would best be resolved by an experiment.

5 CONCLUSIONS

The analysis of the preceding sections together with the numerical examples has demonstrated:

(a) That a certain family of twodimensional flapped aerofoil sections can be constructed using a family of conformal mappings of a circle. The mappings are inspired by the degenerate case, when the resulting aerofoil is a 'skeleton' consisting of a flat plate and a flat plate flap.

(b) That for such an aerofoil the upper surface pressure distribution shows a significant adverse pressure gradient near the flap knee whose magnitude increases with increasing flap deflection.

(c) That by adding suitable fluid source distributions in the outer flow, the adverse pressure gradient for 13.5° and 18° of flap deflection can be made as good as (or better than) that for 9°, with a consequent increase of up to 0.5 in usable C_L.

(d) That on the present theory, the fluid source distribution may be replaced by a certain heat source distribution, without altering the effect on adverse pressure gradients. In the best example considered, an increase of 0.26 in C_L was achieved by increasing the flap deflection and adding heat described by

a specific fuel consumption parameter of value 0.48 lb wt fuel per hour per lb of lift force. This figure is comparable with the specific fuel consumptions of other high lift devices (e.g. fan lift engines).

In view of these results, it is suggested that an increase in the usable C_L of an aerofoil with flap should be possible by adding heat to the external flow above the knee, and so reducing the local adverse pressure gradient and delaying separation. Since the main effect of the heat addition is fairly local it is not thought to be important that the aerofoil used in the examples is untypical of full scale practice, at least in order to demonstrate the principle.

The attraction of the 'heat flap' suggestion is that the heat has a role best described as that of a 'catalyst'. The extra lift is not a direct result of the heat addition (by way of some sort of thrust) which might be expected to require a very great deal of heat, but is strictly associated with an increase in flap deflection. The heat makes the increase possible by retaining an attached boundary layer.

If a practical application is envisaged, however, a number of points need further investigation, e.g.:

(a) more practical aerofoil shapes
(b) the effect of heat on the boundary layer
(c) the modification of the results for finite Mach number
(d) possible use in conjunction with a slotted flap
(e) the practical problems of heat addition in the external flow and of a small amount of momentum addition. If it is not possible to add momentum, what is the modification of the 'heat flap' effect by omitting it?
(f) a project balance sheet in which possible gains through using a 'heat flap' are offset against the penalties introduced by it.

Appendix A

CONFORMAL MAPPING OF THE EXTERIOR OF A CIRCLE ON TO THE EXTERIOR OF A FLAPPED AEROFOIL SECTION

A.1 Basic idea

A skeleton aerofoil consisting of a flat plate with a deflected flat plate flap is first considered, and its outline, which may be regarded as a 'skeleton polygon' (Fig.14a), is mapped onto a unit circle. This is done by first mapping the exterior of the polygon onto an upper half-plane by a Schwarz-Christoffel type transformation (Fig.14b), and then mapping the half-plane onto the exterior of a unit circle (Fig.14c) by a Möbius transformation. These transformations can be arranged so that the points at infinity in the circle and profile planes correspond, and the trailing edge of the profile is mapped onto the point 1 in the circle plane.

Flapped aerofoils of non-zero thickness are now considered by examining the inverse image under the above transformation, of the circle $C(\epsilon)$ (Fig.15a) obtained by 'clothing' the unit circle. This inverse image turns out to be a 'clothing' of the skeleton polygon. Stages in the inversion of the transformation are shown in Figs.15b and c, and some resulting profiles appear in Fig.17. In this Appendix the notation of Figs.14 and 15 is made standard, that is the complex variable z refers to the profile plane, w to the intermediate plane, and ζ to the circle plane.

A.2 The mapping $w \to z$

A.2.1 General remarks about Schwarz-Christoffel transformations

A mapping is required of the region $\mathrm{Im}[w] \geqslant 0$ of the complex w-plane onto the exterior of the profile P_0 (Fig.14a) which is conformal except at a set of four real points (which are to be mapped onto the vertices (1), (2), (3), (4) of the skeleton) and at some point w_0 with $\mathrm{Im}[w_0] > 0$ (which is to be mapped onto the point at infinity in the z-plane). The point w_0 must be introduced explicitly since ∞_z ($= \infty$ in the z-plane) lies in the flow region of the z-plane, and further it is required that $\mathrm{Im}[w_0] \neq 0$ because ∞_z is not a boundary point of that region.

This is a special case of the problem of mapping the region $\mathrm{Im}[w] > 0$ onto the exterior of a finite, simple n-sided polygon in the z-plane, with vertices at $z_1, z_2, \ldots z_n$, viewed in the *clockwise* direction, and with corresponding angles $\alpha_1\pi, \alpha_2\pi, \ldots \alpha_n\pi$ rad, $(\alpha_1 + \alpha_2 + \ldots + \alpha_n = 2)$.

This problem is to be distinguished from the more standard Schwarz-Christoffel problem, which concerns the *interior* of the finite n-gon. Many texts only treat the standard case, but see Markushevich[5] (for example) where the three cases ∞ an exterior point of a finite polygon, ∞ a vertex of an infinite polygon and ∞ an exterior point of a finite polygon (standard) are considered. In the first case, he demonstrates that if f is a mapping with all the properties demanded above then it must satisfy:

$$f'(w) = \frac{A \prod_{i=1}^{n} (w - a_i)^{\alpha_i}}{(w - w_0)^2 (w - \bar{w}_0)^2}$$

where:

(a) The a_i are the inverse images under the mapping f of the corresponding z_i. They are all real, and $a_1 > a_2 > \ldots > a_n$ or cyclic permutations of that statement.

(b) Any three a_i may be arbitrarily selected (as long as the ordering is respected) and the rest are then uniquely determined by the proportions of the sides of the polygon.

(c) w_0 (the inverse of image of ∞ under f) satisfies $\mathrm{Im}[w_0] > 0$ and (important) a condition which ensures that f is a one-valued function on $\mathrm{Im}[w] > 0$. This condition is that f' should have no residue at any point in the upper half plane. The only point of concern is w_0, and so this condition is simply that the coefficient of $1/(w - w_0)$ in the expansion of f' about w_0 be zero.

(d) The complex constant A is determined by the overall scale and orientation of the polygon. Its position in the z-plane fixes a constant of integration.

By applying a certain Möbius transformation to the w-plane, it may be mapped onto a w*-plane (say) in such a way that the two upper half planes correspond, and any one of the a_i is mapped onto ∞_{w^*}. This transformation may be combined with f to produce a mapping f^* of the w*-plane onto the z-plane, satisfying:

$$f^{*\prime}(w^*) = \frac{A^* \prod_{i=1}^{n-1} (w^* - a_i^*)^{\alpha_i}}{(w^* - w_0^*)^2 (w^* - \bar{w}_0^*)^2} \qquad \text{(A-1)}$$

where it has been chosen to map a_n onto ∞_{w^*} and the notation:

$$a_1 \to a_i^* \quad , \quad w \to w^* \quad , \quad A \to A^*$$

has been used. In the sequel the w*-plane is used directly and the * suppressed.

A.2.2 Transformation of the skeleton polygon[6,7]

An appropriate form of equation (A-1) for the skeleton polygon is

$$f'(w) = \frac{A(w - 1)(w + X)w^{-\alpha}}{(w - w_0)^2 (w - \bar{w}_0)^2} \qquad \text{(A-2)}$$

where $\alpha\pi$ = flap deflection angle, and the following correspondences have been chosen:

vertex (1) → 1
vertex (2) → ∞_w
vertex (3) → -X
vertex (4) → 0 (see Fig.14) .

The conditions (a)-(d) of A.2.1 become:

(a) $X > 0$ (images of (1), (2), (4) have been fixed).

(b) X is determined by the parameter δ = ratio of flap chord length to L (Fig.14a).

(c) Closure condition (see below).

(d) A is fixed by the parameter L and the orientation of the polygon.

The integration constant is fixed by noting that $f(0) = 0$, so that

$$f(w) = A \int_0^w \frac{(t - 1)(t + X)t^{-\alpha}}{(t - w_0)^2 (t - \bar{w}_0)^2} \, dt \quad .$$

Remarkably, this integral can be performed analytically, provided the closure condition (c) is imposed. The result of the integration is here stated, and the condition (c) deduced from a verification by differentiation.

Consider

$$f(w) = -\frac{Aw^{1-\alpha}/(1+\alpha)}{(w-w_0)(w-\bar{w}_0)}$$

so that

$$f'(w) = \frac{A\left[w^2 - \frac{\alpha}{1+\alpha}(w_0+\bar{w}_0) - \frac{1-\alpha}{1+\alpha}w_0\bar{w}_0\right]w^{-\alpha}}{(w-w_0)^2(w-\bar{w}_0)^2} \quad .$$

This is precisely of the form of equation (A-2) if:

$$\left.\begin{aligned} 1 - X &= \frac{\alpha}{1+\alpha}(w_0+\bar{w}_0) \\ \text{and} \qquad X &= \frac{1-\alpha}{1+\alpha}w_0\bar{w}_0 \end{aligned}\right\} \quad . \qquad \text{(A-3)}$$

These two equations amount to one complex condition on w_0 when X is eliminated, and this is the closure condition (c) previously discussed. The condition $f(0) = 0$ is respected.

A.2.3 Matching parameters

The remaining constants are fixed by the demands: $f(1) = -L$ and $f(-X) = \delta L \exp(-i\alpha\pi)$. The first becomes, on applying the closure condition (A-3):

$$\frac{-A\alpha(1-\alpha)/(1+\alpha)}{(1-\alpha)-(1+\alpha)X} = L \quad . \qquad \text{(A-4)}$$

The second, after similar manipulation becomes:

$$\frac{-A\alpha(1-\alpha)(-X)^{-\alpha}/(1+\alpha)}{(1+\alpha)-(1-\alpha)X} = -\delta L \exp(-i\alpha\pi) \quad . \qquad \text{(A-5)}$$

After division of (A-5) by (A-4), there obtains:

$$X^{-\alpha}\,\frac{(1-\alpha)-(1+\alpha)X}{(1-\alpha)X-(1+\alpha)} \;=\; \delta$$

or, denoting

$$(1-\alpha)/(1+\alpha) \;=\; \beta \quad , \quad (\beta - X)/(\beta X - 1) \;=\; \delta X^{\alpha} \quad . \qquad \text{(A-6)}$$

Graphical analysis (Fig.16) shows that this equation has a unique solution which satisfies $0 < \beta < X < 1/\beta$*, for all positive δ, and $0 < \alpha < 1$. The solution may be obtained numerically.

Finally from (A-4),

$$A \;=\; -L(1+\alpha)[(1-\alpha)-(1+\alpha)X]/\alpha(1-\alpha) \;=\; -L(1+\alpha)(\beta - X)/\alpha\beta \quad .$$

The whole transformation is thus determined.

A.3 The mapping $\zeta \to w$

This is a standard, Möbius transformation defined by the demands that w_0 and ∞_ζ are to correspond, and the point $w = -X$ is to correspond with $\zeta = 1$. The required mapping is

$$w \;=\; g(\zeta) \;=\; \frac{\zeta w_0 - K\bar{w}_0}{\zeta - K}$$

where $K = (X + w_0)/(X + \bar{w}_0)$.

A.4 Summary

The exterior of the circle $|\zeta| = 1$, is mapped onto the exterior of the polygonal curve P_0, by the mapping fg, where

---

* From equations (A-3), $\{\mathrm{Im}[w_0]\}^2 = \frac{1+\alpha}{1-\alpha}X - \frac{1}{4}\frac{(1+\alpha)^2(1-X)^2}{\alpha^2}$.
It is clearly necessary that this expression be positive, and the condition for this may be shown to be $\beta < X < 1/\beta$.

$$g(\zeta) = \frac{\zeta w_0 - K\bar{w}_0}{\zeta - K} \quad ,$$

$$f(w) = \frac{Aw^{1-\alpha}/(1+\alpha)}{(w - w_0)(w - \bar{w}_0)}$$

X is the unique solution satisfying $\beta < X < 1/\beta$ of

$$\delta X^{\alpha} = (\beta - X)/(\beta X - 1) \quad ,$$

and $$w_0\bar{w}_0 = X/\beta \quad , \quad w_0 + \bar{w}_0 = (1 - X)(1 + \alpha)/\alpha \quad , \quad \mathrm{Im}[w_0] > 0 \quad ,$$

$$A = -L(1 + \alpha)(\beta - X)/\alpha\beta \quad ,$$

$$\beta = (1 - \alpha)/(1 + \alpha) \quad ,$$

$$K = (X + w_0)/(X + \bar{w}_0) \quad .$$

A.5 The 'clothed' aerofoil

The final step in constructing the aerofoil is to examine the image under $F = fg$ of the 'clothed' circle $C(\varepsilon)$, defined to have centre at $\zeta = -\varepsilon$ and radius $1 + \varepsilon$, so that it passes through $\zeta = 1$ but otherwise lies strictly outside the unit circle. This means that the image curve will be closed, and will have a continuously turning tangent except at the point corresponding to $\zeta = 1$ (the trailing edge) where there is a singularity the same as that of the skeleton. The trailing edge angle of the 'clothed' aerofoil will thus be zero. Beyond this, it is necessary to turn to computation to discover the detailed shape. An aerofoil so produced, is defined by the parameters $L, \delta, \alpha, \varepsilon$ and this profile is referred to as $P(L, \delta, \alpha, \varepsilon)$. Some resulting profiles are shown in Fig.17.

A.6 Derivatives of the transformation F

(a) $$F'(\zeta) = f'(w)g'(\zeta) = \frac{A(w - 1)(w + X)w^{-\alpha}}{(w - w_0)^2(w - \bar{w}_0)^2} \frac{K(\bar{w}_0 - w_0)}{(\zeta - K)^2}$$

$$= -\frac{A(w - 1)(w + X)w^{-\alpha}}{K(w_0 - \bar{w}_0)(w - \bar{w}_0)^2}$$ when the results of

(A-5) are applied. In particular,

$$F'(1) = 0$$

and

$$F'(\infty) = -\frac{A(w_0 - 1)(w_0 + X)w_0^{-\alpha}}{K(w_0 - \bar{w}_0)^3}$$

$$= \Lambda \quad \text{(say)} \quad .$$

(b) As required in Appendix B,

$$\frac{d}{d\zeta}\left[\log F'(\zeta)\right] = \left[\frac{1}{w - 1} + \frac{1}{w + X} - \frac{\alpha}{w} - \frac{2}{w - \bar{w}_0}\right]\frac{dw}{d\zeta}$$

$$= \left[\frac{1}{w - 1} + \frac{1}{w + X} - \frac{\alpha}{w} - \frac{2}{w - \bar{w}_0}\right]\frac{K(\bar{w}_0 - w_0)}{(\zeta - K)^2} \quad .$$

Appendix B

THE RELATIONSHIP BETWEEN PROFILE PLANE AND CIRCLE PLANE FLOWS, AND THE DETERMINATION OF THE LATTER

B.1 The relationship

According to incompressible, irrotational, inviscid, flow theory, the flow around the profile $P(L,\delta,\alpha,\varepsilon)$ fixed by the data discussed in section 3.2 may be inferred from a certain flow in the region D of the ζ-plane, using the method of complex potential. The complex potential $W(z)$ is analytic except at singularities of the flow, and satisfies $dW/dz = \bar{V}(z)$ where V is the complex velocity and the bar denotes complex conjugate function. The function $\Omega(\zeta) = W(F(\zeta))$ is the complex potential of a flow in D which satisfies:

(a) The rigid surface boundary condition on $C(\varepsilon)$.

(b) If $\nu(\zeta) = \overline{d\Omega/d\zeta}$ (= complex velocity in the ζ-plane) and $V(z) \to V_0$ as $z \to \infty$, then $\nu(\zeta) \to \nu_0 = \bar{\Lambda}V_0$ as $\zeta \to \infty$.

(c) The ζ and z plane flows have the same circulation κ and the same source-type singularities and distributions (of same strengths) at corresponding points by the mapping F. In the case of a source distribution $\mu(\zeta)$ in the ζ-plane, the corresponding z-plane distribution is $m(z) = \mu(F^{-1}(z))$. Higher order singularities have a more complicated relationship but are not relevant here.

This ζ-plane problem may be solved by the use of the circle theorem (see e.g. Ref.8) or, in the case of source flow, the method of images. The circulation is fixed by Joukowski's hypothesis which requires the velocity to be zero at $\zeta = 1$. When Ω and $\bar{\nu}$ have been determined, the corresponding quantities W and $\bar{V}$ follow by the relations:

$$W(z) = \Omega(\zeta) \qquad \bar{V}(z) = \bar{\nu}(\zeta)/F'(\zeta) \qquad (F(\zeta) = z) \quad .$$

B.2 The functions Ω, $\bar{\nu}$ and κ

(a) No singularities in the free stream

$$\Omega(\zeta) = \bar{\nu}_0(\zeta + \varepsilon) + \nu_0 \frac{(1 + \varepsilon)^2}{\zeta + \varepsilon} + (\nu_0 - \bar{\nu}_0)(1 + \varepsilon) \log (\zeta + \varepsilon)$$

a function to be referred to as $\Omega_f(\zeta)$ (f = 'free of sources'),

$$\bar{v}(\zeta) = \bar{v}_0 - v_0\left(\frac{1+\varepsilon}{\zeta+\varepsilon}\right)^2 + (v_0 - \bar{v}_0)\left(\frac{1+\varepsilon}{\zeta+\varepsilon}\right) = \bar{v}_f(\zeta)$$

$$\kappa = 4\pi(1+\varepsilon)\mathrm{Im}[v_0] = \kappa_f \quad .$$

(b) A single point source of strength m at the point ζ^* in $D(\varepsilon)$, with $\mathrm{Im}[\zeta^*] > 0$

$$\Omega(\zeta) = \Omega_f(\zeta) + \frac{m}{2\pi}\left\{\log(\zeta-\zeta^*) + \log\left[\frac{(1+\varepsilon)^2}{\zeta+\varepsilon} - (\bar{\zeta}^*+\varepsilon)\right] - \frac{(\zeta-\zeta^*)}{|1-\zeta^*|^2}(1+\varepsilon)\log(\zeta+\varepsilon)\right\}$$

$$= \Omega_f(\zeta) + m\Omega[\zeta^*,\zeta]$$

$$\bar{v}(\zeta) = \bar{v}_f(\zeta) + \frac{m}{2\pi}\left\{\frac{1}{\zeta-\zeta^*} - \frac{\bar{\zeta}^*+\varepsilon}{(1+\varepsilon)^2 - (\bar{\zeta}^*+\varepsilon)(\zeta+\varepsilon)} - \frac{1}{\zeta-\varepsilon} - \frac{\zeta-\zeta^*}{|1-\zeta^*|^2}\frac{1+\varepsilon}{\zeta+\varepsilon}\right\}$$

$$= \bar{v}_f(\zeta) + m\bar{v}[\zeta^*,\zeta]$$

$$\kappa = \kappa_f - \frac{2m(1+\varepsilon)\mathrm{Im}[\zeta^*]}{|1-\zeta^*|^2}$$

$$= \kappa_f + m\kappa[\zeta^*] \quad .$$

Since for $\mathrm{Im}[\zeta^*] > 0$, $\kappa[\zeta^*] < 0$, the immediate effect of adding a source is to reduce the circulation and so cut down lift.

(c) The complex potential for several point sources or a source distribution consists of the basic function $\Omega_f(\zeta)$ and a sum or integral over ζ^* of the functions $\mu(\zeta^*)\Omega[\zeta^*,\zeta]$, where $\mu(\zeta^*)$ is the point source strength at ζ^* or source density at ζ^* respectively. Similar expressions hold for $\bar{v}$ and κ.

B.3 Pressure gradients

In making decisions on boundary layer separation, the derivative of C_p around the surface of the aerofoil is required. If s is the coordinate measured around the profile from the trailing edge, the function of interest is $G(s) = -d(C_p)/ds$, i.e. the adverse pressure gradient. This is calculated as follows:

$$G(s) = -d(C_p)/ds = d(V\bar{V}/U_0^2/ds \quad .$$

Suppose the point s corresponds to the point $\zeta = (1 + \varepsilon)\exp(i\theta) - \varepsilon$ on $C(\varepsilon)$. Treating θ as a new coordinate, one obtains:

$$(1 + \varepsilon)d\theta/ds = |d\zeta/dz| = 1/|F'(\zeta)| \quad .$$

Thus

$$G(s) = \frac{d(V\bar{V})/d\theta}{U_0^2(1 + \varepsilon)|F'(\zeta)|}$$

$$d(V\bar{V})/d\theta = 2\mathrm{Re}[Vd\bar{V}/d\theta]$$

$$d\bar{V}/d\theta = (1 + \varepsilon)i\exp(i\theta)d\bar{V}/d\zeta$$

$$d\bar{V}/d\zeta = [F'(\zeta)d\bar{\nu}/d\zeta - \bar{\nu}(\zeta)dF'/d\zeta]/[F'(\zeta)]^2$$

$$= [\chi(\zeta) - \bar{\nu}d(\log F')/d\zeta]/F'(\zeta)$$

where $\chi(\zeta) = d\bar{\nu}/d\zeta$.

Thus one obtains:

$$G(s) = -\frac{2}{U_0^2|F'(\zeta)|^3}\,\mathrm{Im}\left[\exp(i\theta)\nu\left\{\chi - \bar{\nu}\frac{d}{d\zeta}(\log F')\right\}\right] \quad .$$

For the cases dealt with in section B.2, χ takes the forms:

(a) $2\nu_0(1 + \varepsilon)^2/(\zeta + \varepsilon)^3 - (\nu_0 - \bar{\nu}_0)(1 + \varepsilon)/(\zeta + \varepsilon)^2 = \chi_f(\zeta)$ (say) .

(b) $$\chi_f(\zeta) + \frac{m}{2\pi}\left\{-\frac{1}{(\zeta-\zeta^*)^2} - \left[\frac{\bar{\zeta}^*+\varepsilon}{(1+\varepsilon)^2-(\bar{\zeta}^*+\varepsilon)(\zeta+\varepsilon)}\right]^2 + \frac{1}{(\zeta+\varepsilon)^2} + \frac{\zeta^*-\bar{\zeta}^*}{|1-\zeta^*|^2}\frac{1+\varepsilon}{(\zeta+\varepsilon)^2}\right\}$$

$$= \chi_f(\zeta) + m\chi[\zeta^*,\zeta] \quad .$$

(c) χ_f plus a sum or integral over ζ^* of $\mu(\zeta^*)\chi[\zeta^*,\zeta]$.

The function $d(\log F')/d\zeta$ is computed in Appendix A.

Appendix C

A SYSTEMATIC, NUMERICAL METHOD FOR THE REDUCTION OF ADVERSE PRESSURE GRADIENTS

In this Appendix, the problem set up in section 3.3 is approached in a systematic way which may be carried out completely on a computer. The success of the method in all circumstances cannot be guaranteed, but it has worked satisfactorily in a number of cases.

A segment Σ of the upper surface of the profile is selected, along which it is required to reduce the maximum adverse pressure gradient to a quoted value G°. The segment Σ must not extend too far forward along the profile as it will encounter regions where the boundary layer is thinner and can therefore withstand greater adverse pressure gradients. Neither must it extend right to the trailing edge near which numerical investigation shows that large adverse pressure gradients inevitably exist, even for very small flap deflections. It is assumed that the resulting separation very close to the trailing edge appreciably distorts the external solution only in a thin wake.

The location s_0 of the maximum value of $G(s)$ on Σ is determined and then a single point source is added in such a way as to reduce the adverse pressure gradient at s_0 to G°. This is done by making use of the following algorithm. Let the suffix u (unmodified) refer to the situation before the source is added (initially u has the same meaning as f in Appendix B), and the suffix m (modified) the situation after the source is added. If the source has strength m and is located at $z^* = F(\zeta^*)$, (assumed to be close to Σ), then:

$$\bar{\nu}_m(\zeta) = \bar{\nu}_u(\zeta) + m\bar{\nu}[\zeta^*,\zeta]$$

$$\chi_m(\zeta) = \chi_u(\zeta) + m\chi[\zeta^*,\zeta] \quad .$$

Substituting these in the expression for $G(s)$ obtained in Appendix B (B.3) one finds:

$$G_m(s) = A_0[\zeta^*,\zeta] + mA_1[\zeta^*,\zeta] + m^2A_2[\zeta^*,\zeta]$$

where each A_1 is real, and explicitly:

$$A_0 = -2\mathrm{Im}\left[\exp(i\theta)\nu_u\left\{\chi_u - \bar{\nu}_u \frac{d}{d\zeta}(\log F')\right\}\right] \Big/ U_0^2 |F'(\zeta)|^3$$

$$= G_u(s)$$

$$A_1 = -2\mathrm{Im}\left[\exp(i\theta)\left\{\nu[\zeta^*,\zeta]\left\{\chi_u - \bar{\nu}_u \frac{d}{d\zeta}(\log F')\right\} + \nu_u\left\{\chi[\zeta^*,\zeta] - \bar{\nu}[\zeta^*,\zeta]\frac{d}{d\zeta}(\log F')\right\}\right\}\right] \Big/ U_0^2 |F'(\zeta)|^3$$

$$A_2 = -2\mathrm{Im}\left[\exp(i\theta)\nu[\zeta^*,\zeta]\left\{\chi[\zeta^*,\zeta] - \bar{\nu}[\zeta^*,\zeta]\frac{d}{d\zeta}(\log F')\right\}\right] \Big/ U_0^2 |F'(\zeta)|^3$$

Suppose now that the point $s = s_0$, $h = 0$ corresponds with $\zeta = (1 + \varepsilon)\exp(i\theta) - \varepsilon$. The procedure is to add a source at $\zeta^* = (1 + \varepsilon + \eta)\exp(i\theta) - \varepsilon$ (where η is a preselected positive parameter fixing the height above the aerofoil at which the source is added). Having so fixed ζ^*, the required source strength is determined by demanding $G_m(s_0) = G^o$, or

$$A_2 m^2 + A_1 m + A_0 - G^o = 0 \quad .$$

The new adverse pressure gradient so obtained satisfies $G_m(s_0) = G^o$, but it is possible that $G_m(s) > G^o$ at some other points s in Σ. The process is therefore repeated taking as unmodified functions (u) the functions previously suffixed (m) and adding a suitable source close to the new maximum of $G_u(s)$. The process is continued until a subsequent function $G_m(s)$ is smaller than G^o everywhere on Σ.

The method is a relaxation process, but one which is so physically inspired that a mathematical convergence proof is virtually impossible. Convergence properties are likely to depend on the parameter η and on the form of the initial unmodified distribution. It is assumed at each stage that the quadratic equation has a real, positive solution. On physical grounds, one would expect this to be true since one always has $A_0 - G^o > 0$. Certainly by adding a source of sufficient strength, the local adverse pressure gradient $G_u(s_0)$ $(= A_0)$ can be reduced to an arbitrary extent, so the existence of one real, positive solution is assured. To cover the possibility of the appearance of two positive sources, a routine can be incorporated to choose the smaller (say).

The chief drawback of the systematic method is that it tends to produce very irregular source distributions, unless, as is often the case, a small number of well chosen sources is adequate.

SYMBOLS

A	area of streamtube which encounters source distribution
c	chord length
C	circle
C_F	specific fuel consumption parameter
C_{LQ}	increment in lift coefficient due to 'heat flap'
D	region outside C
F	mapping from circle plane to profile plane
G	adverse pressure gradient
h	height coordinate above profile
H	calorific value of fuel
L	length of profile from leading edge to flap knee
m	point fluid source strength or distribution function
M	Mach number
p	pressure
P	profile curve
Q	total heat source strength
r	polar coordinate in circle plane
R	source region
s	coordinate measured around upper surface of profile from trailing edge
S	streamtube which encounters source distribution
t	duration of use of 'heat flap', and time
U	flow speed (profile plane)
V	complex velocity (profile plane)
w	complex variable (intermediate plane)
W	complex velocity potential (profile plane)
z	complex variable (profile plane)
α	$\alpha\pi$ = flap deflection angle in radians
γ	ratio of specific heats
δ	ratio flap chord length to L
ϵ	'thickness parameter'
ζ	complex variable (circle plane)
θ	polar coordinate in circle plane
κ	circulation
Λ	$\lim_{\zeta\to\infty} F'(\zeta)$

SYMBOLS (concluded)

μ	fluid source distribution
ν	complex velocity (circle plane)
ρ	density
χ	$d\bar{\nu}/d\zeta$
Ω	complex velocity potential (circle plane)

REFERENCES

No.	Author	Title, etc.
1	E.G. Broadbent	A theoretical exploration of the flow about an electric arc transverse to an airstream using potential flow methods. ARC R & M 3531 (1965)
2	E.G. Broadbent	High lift by heat addition to the flow. Private communication (1969)
3	J.B. Edwards	Private communication (1971)
4	P.D. Smith	A note on the computation of the inviscid rotational flow past the trailing edge of an aerofoil. Unpublished MOD(PE) material
5	A.I. Markushevich	Theory of functions of a complex variable. Vol.III, English translation; Prentice Hall (1967)
6	F. Keune	Auftrieb einer geknickten eben Platte. Luftfahrt Forschung, 13, 85 (1936)
7	A. Cheers	M.Phil Thesis, Southampton University
8	G.K. Batchelor	An introduction to fluid dynamics. Cambridge University Press (1967)

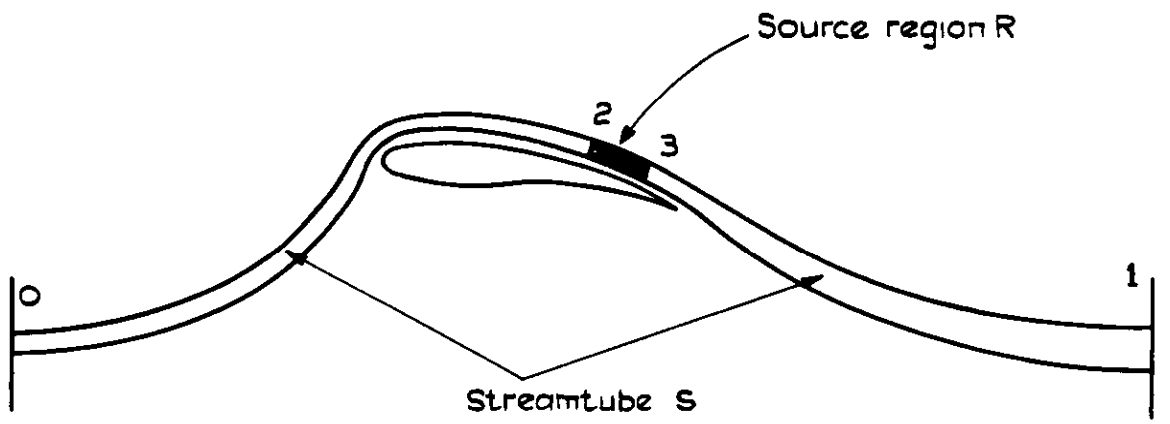

Fig. 1 The expanded streamtube

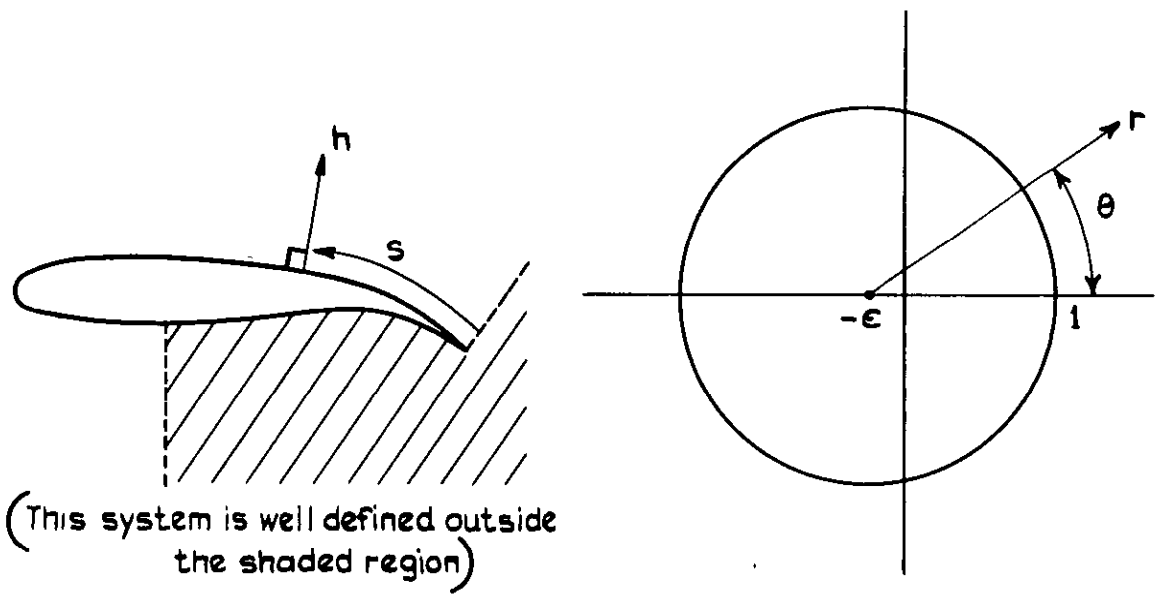

Fig.2 Coordinate systems in profile and circle planes

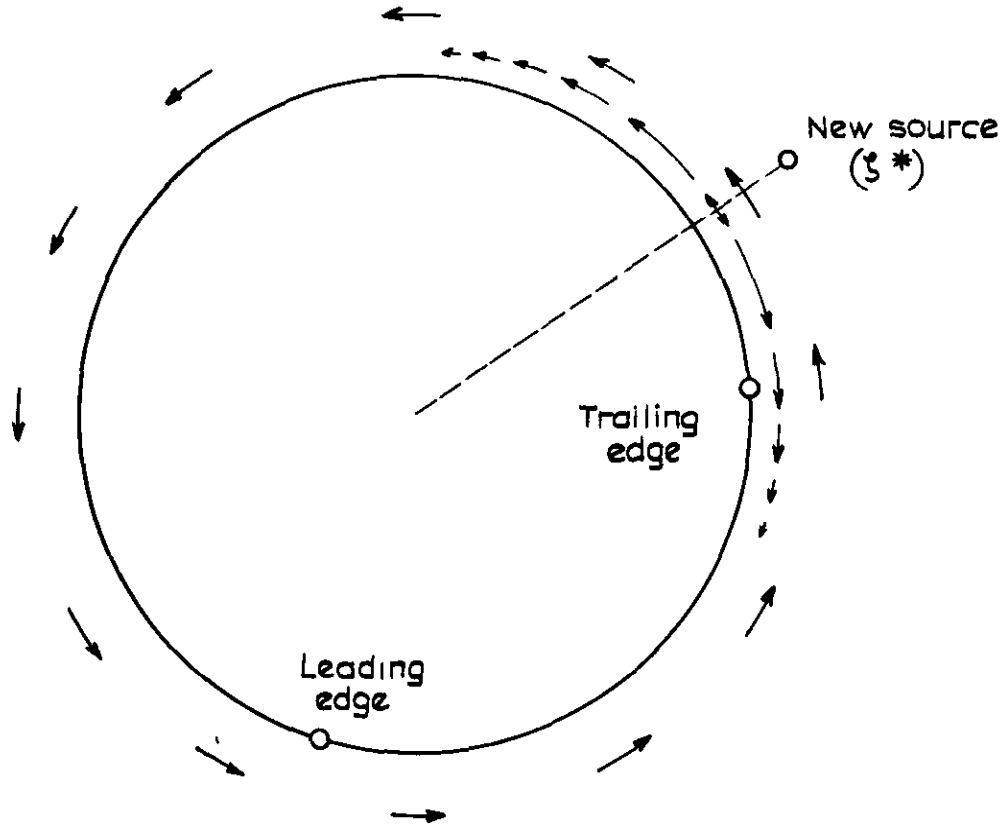

The additional velocities induced by the new source are shown by arrows. There are two arrow chains: one is the "direct" effect of the source and its image and to this is added an anticlockwise circulation to restore the Joukowski condition at the trailing edge. Magnitude of velocity is represented by arrow length

Fig.3 Effect on circle plane flow of adding a single point source (with its image and additional circulation)

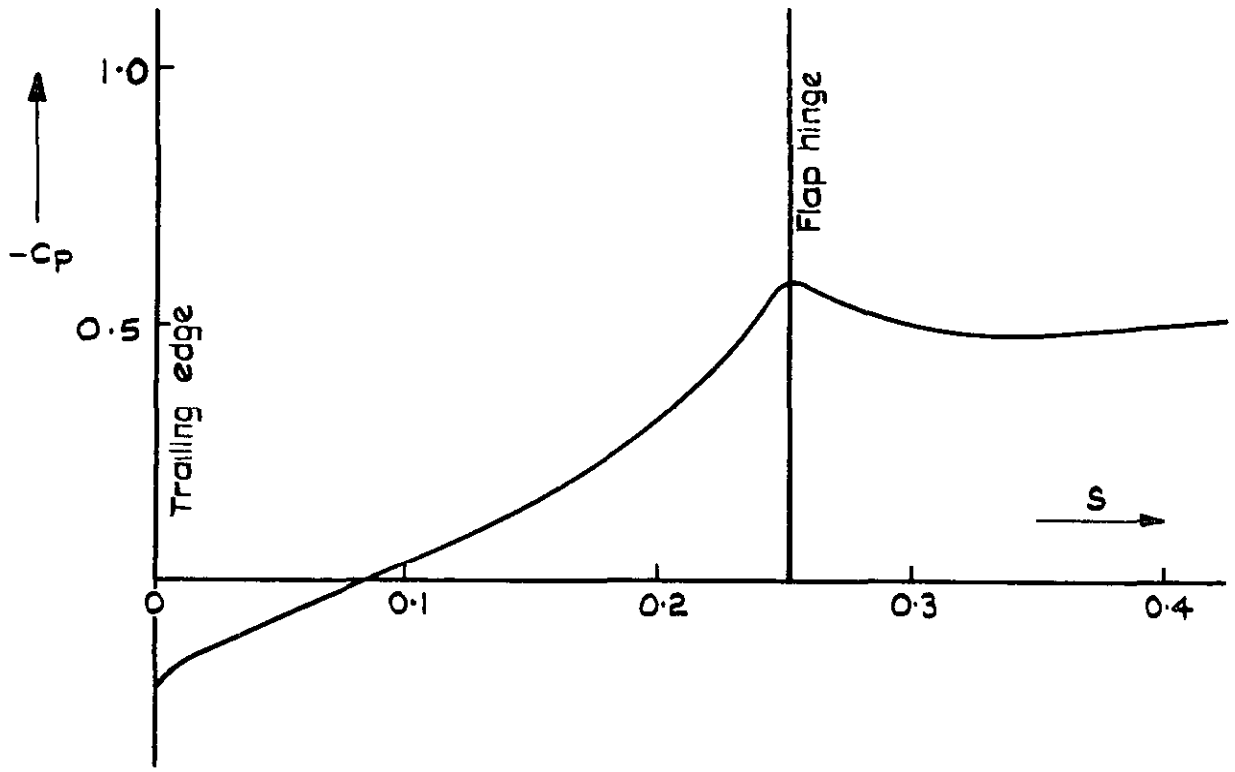

Profile P(1·0, 0·25, 0·05, 0·1) (flap angle 9°)

For flow $U_0 = 1·0$ angle of attack = $0·05\pi$ rad $(\simeq 9°)$

Lift coefficient 1·67

Max flap adverse pressure gradient 6·16

Fig. 4 Pressure distribution over the rearward upper surface in the datum condition

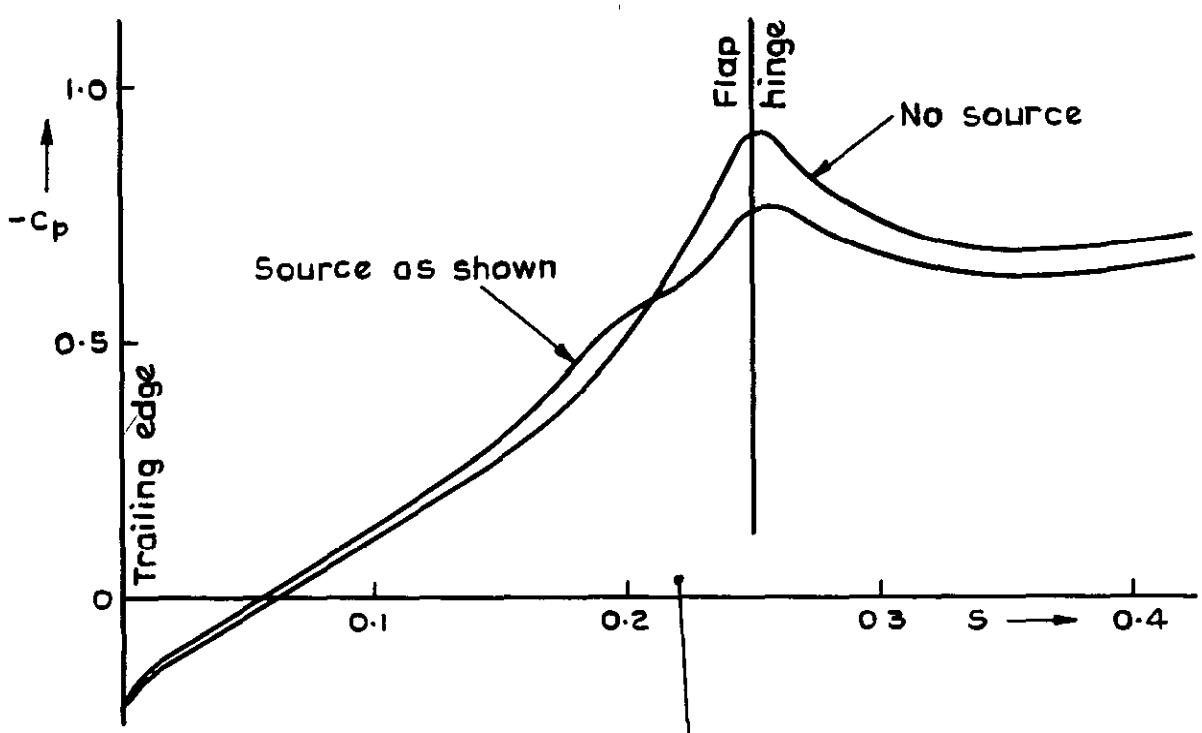

h	0·0394
R	1·2
θ	48°
m	0·01

Profile P (1·0, 0·25, 0·075, 0·1) (flap angle 13·5°)

Far flow $U_0 = 1·0$, angle of attack = $0·05\pi$ rad ($\simeq 9°$)

	No source	Source as shown
Lift coefficient	1·96	1·92
Max flap adverse pressure gradient	10·34	5·65

$U_0 C_F = 0·014$ $C_{LQ} = 0·25$

Fig.5 First comparison case pressure curves
First solution — trial and error

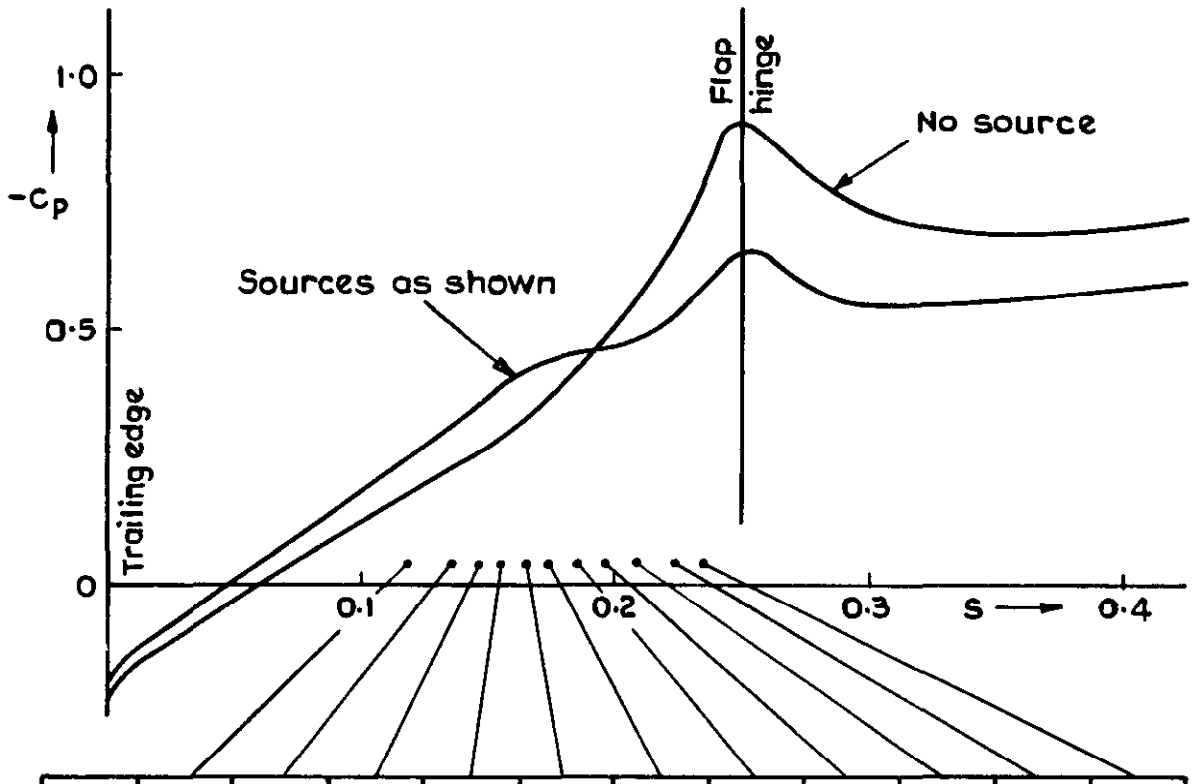

h	0·033	0·035	0·036	0·0365	0·0376	0·038	0·0386	0·0389	0·0393	0·0394	0·0392
R	1·2	1·2	1·2	1·2	1·2	1·2	1·2	1·2	1·2	1·2	1·2
θ	33°	36°	37·5°	39°	40·5°	42°	43·5°	45°	46·5°	48°	49·5°
m	0·0005	0·0005	0·0005	0·001	0·001	0·002	0·002	0·002	0·003	0·005	0·003

Profile P (1·0, 0·25, 0·075, 0·1) (flap angle 13·5°)
Far flow $U_0 = 1·0$, angle of attack $= 0·05\pi$ rad ($\simeq 9°$)

	No source	Sources as shown
Lift coefficient	1·96	1·88
Max flap adverse pressure gradient	10·34	5·56

$U_0 C_F = 0·047$ $\qquad$ $C_{LQ} = 0·21$

Fig.6 First comparison case pressure curves
Second solution — trial and error

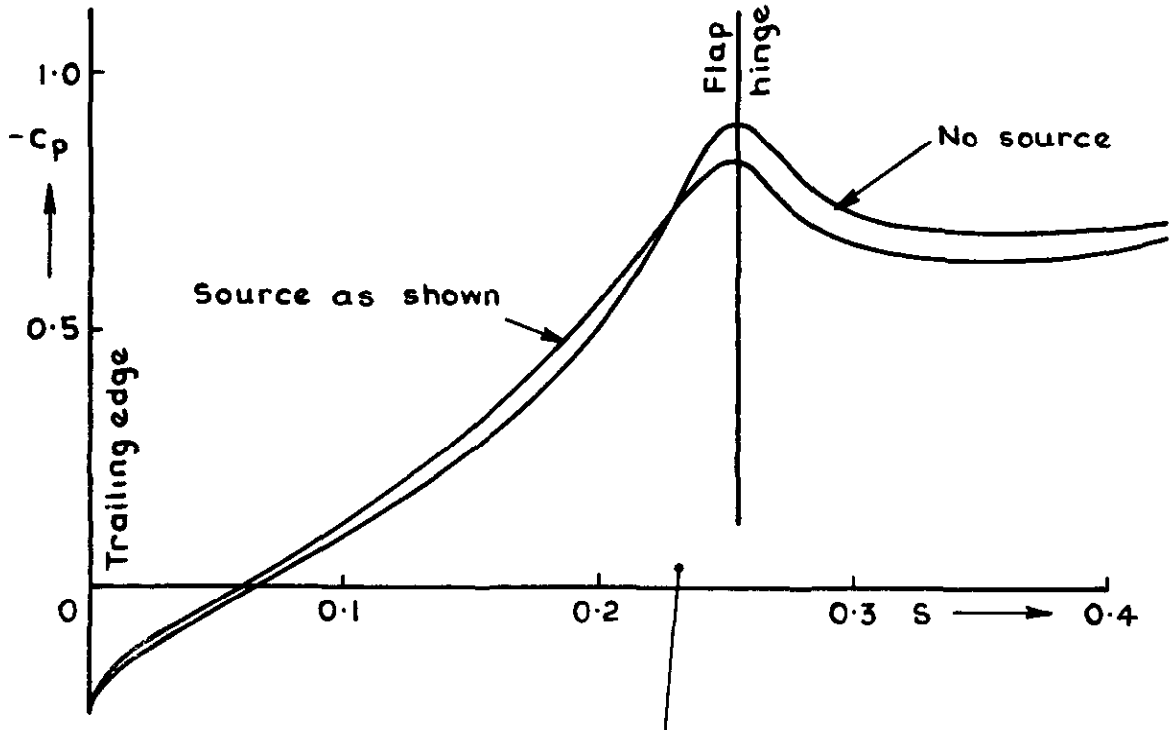

h	0 0392
R	1 2
θ	49·5°
m	0·0069

Profile P(1 0, 0·25, 0·075, 0 1) (flap angle 13·5°)

Far flow $U_0 = 1\ 0$, angle of attack = $0{\cdot}05\ \pi$ rad $(\simeq 9°)$

	No source	Source as shown
Lift coefficient	1 96	1·93
Max flap adverse pressure gradient	10·34	6·16

$U_0 C_F = 0\ 008$ $C_{LQ} = 0{\cdot}26$

Fig. 7 First comparison case pressure curves
Third solution – systematic

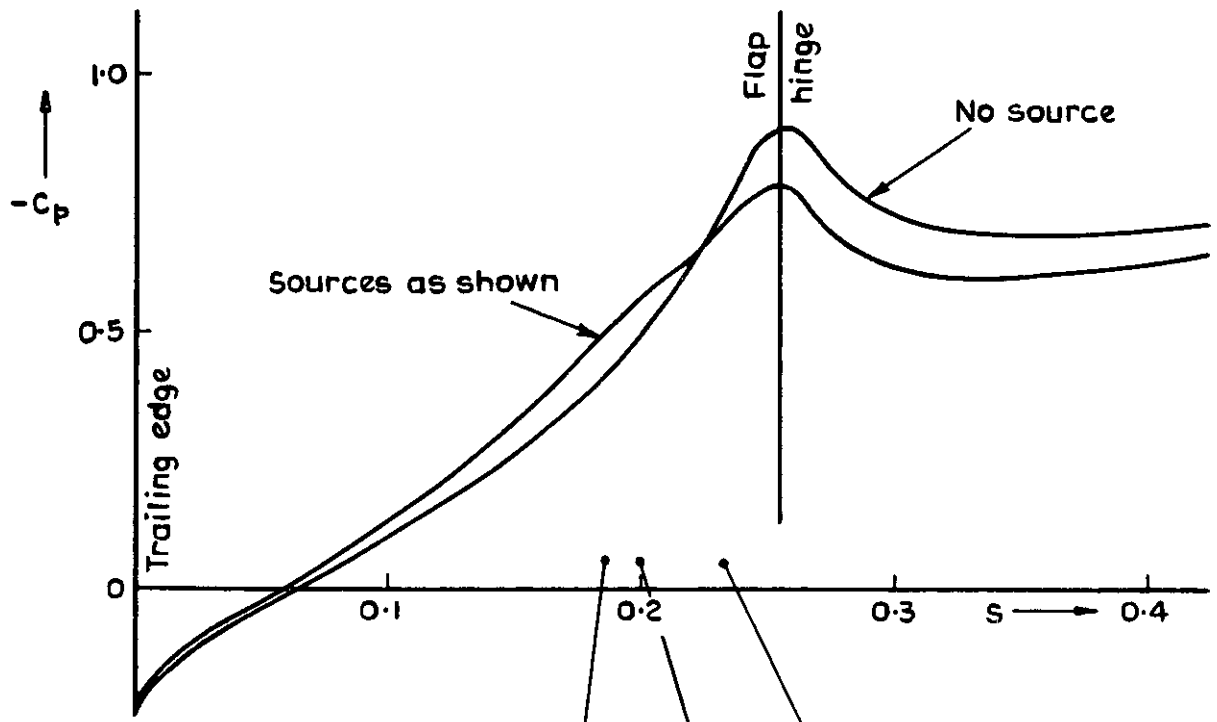

h	0·0386	0·0389	0·0392
R	1·2	1·2	1·2
θ	43·5°	45°	49·5°
m	0·00002	0·0013	0·0088

Profile P(1·0, 0·25, 0·075, 0·1) (flap angle 13·5°)

Far flow $U_0 = 1·0$, angle of attack = $0·05\pi$ rad ($\simeq 9°$)

	No source	Sources as shown
Lift coefficient	1·96	1·915
Max flap adverse pressure gradient	10·34	5·00

$U_0 C_F = \cdot 014$ $C_{LQ} = 0·245$

Fig. 8 First comparison case pressure curves
Fourth solution — systematic

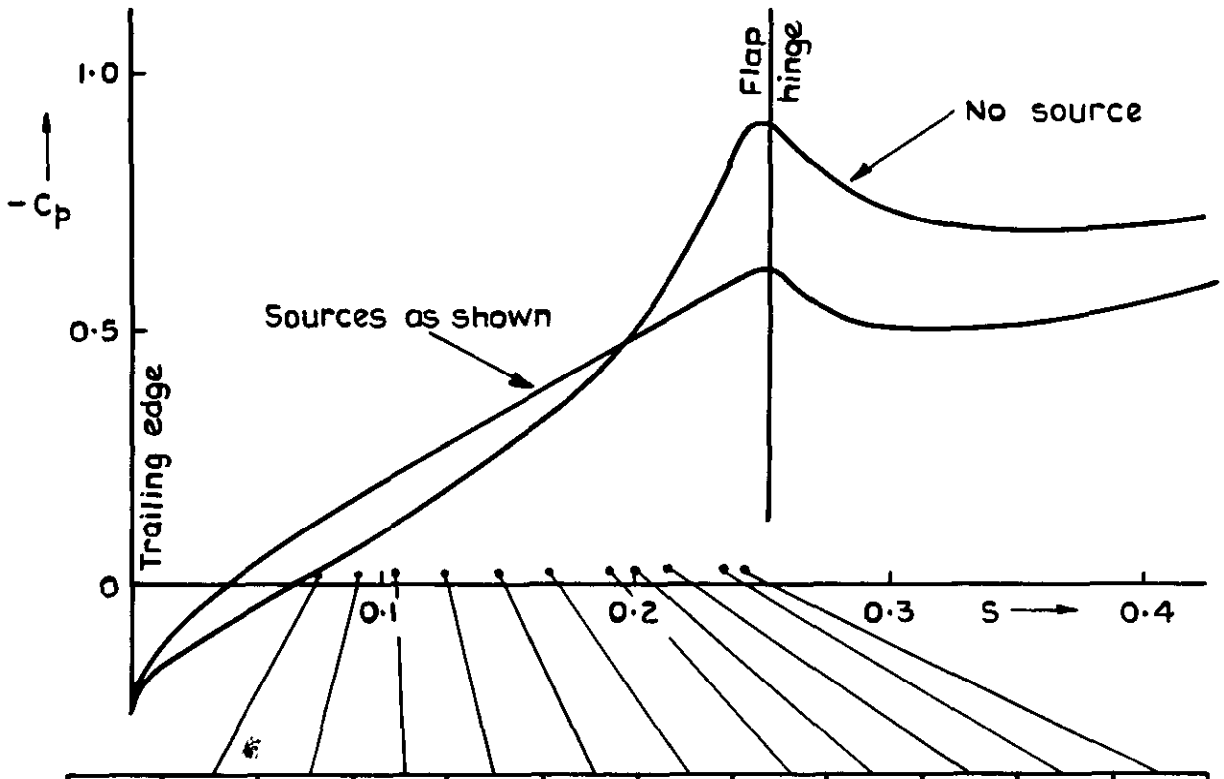

h	0·03	0·031	0·033	0·034	0·036	0·038	0·0386	0·0389	0·0393	0·0392	0·0391
R	1·2	1·2	1·2	1·2	1·2	1·2	1·2	1·2	1·2	1·2	1·2
θ	25·5°	28·5°	31·5°	34·5°	37·5°	40·5°	43·5°	45°	46·5°	49·5°	51°
m	0·00066	0·00041	0·0012	0·00087	0·0024	0·0027	0·0048	0·000018	0·0019	0·012	0·00078

Profile P (1·0, 0·25, 0·075, 0·1) (flap angle 13·5°)

Far flow $U_0 = 1·0$, angle of attack = 0·05 π rad ($\simeq 9°$)

	No sources	Sources as shown
Lift coefficient	1·96	1·83
Max flap adverse pressure gradient	10·34	3·006

$U_0 C_F = 0·104$ $C_{LQ} = 0·16$

Fig. 9 First comparison case pressure curves
Fifth solution — systematic

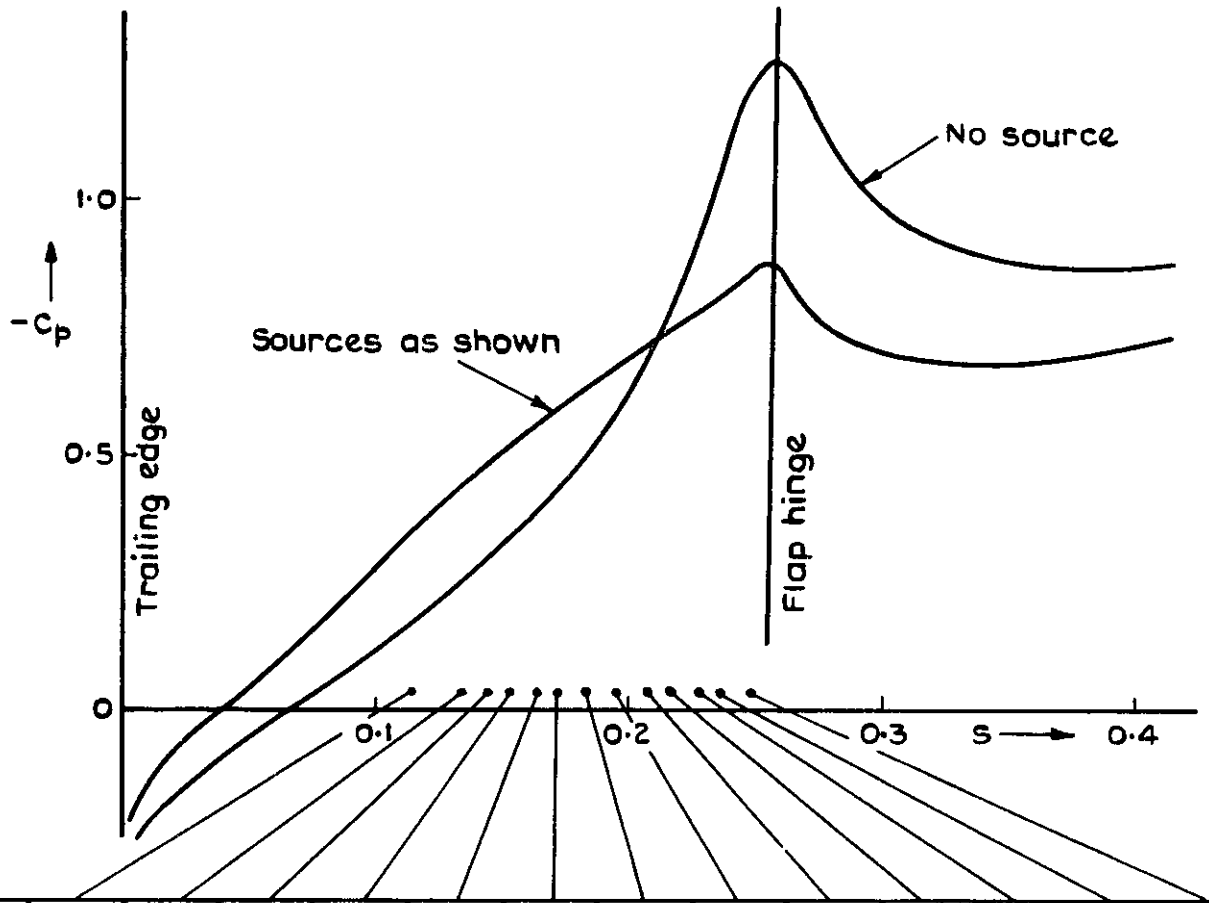

h	0·032	0·034	0·035	0·036	0·037	0·037	0·037	0·037	0·037	0·037	0·037	0·037	0·037
R	1·2	1·2	1·2	1·2	1·2	1·2	1·2	1·2	1·2	1·2	1·2	1·2	1·2
θ	33°	36°	37·5°	39°	40·5°	42°	43·5°	45°	46·5°	48°	49·5°	51°	52·5°
m	0·0005	0·0005	0·001	0·0015	0·0015	0·0015	0·0015	0·0015	0·002	0·005	0·006	0·006	0·001

Profile P (1·0, 0·25, 0·1, 0·1) (flap angle 18°)

Far flow $U_0 = 1·0$, angle of attack = $0·05\pi$ rad ($\simeq 9°$)

	No source	Sources as shown
Lift coefficient	2·25	2·14
Max flap adverse pressure gradient	15·58	6·15

$U_0 C_F = 0·046$ $C_{LQ} = 0·47$

Fig.10 Second comparison case pressure curves
First solution — trial and error

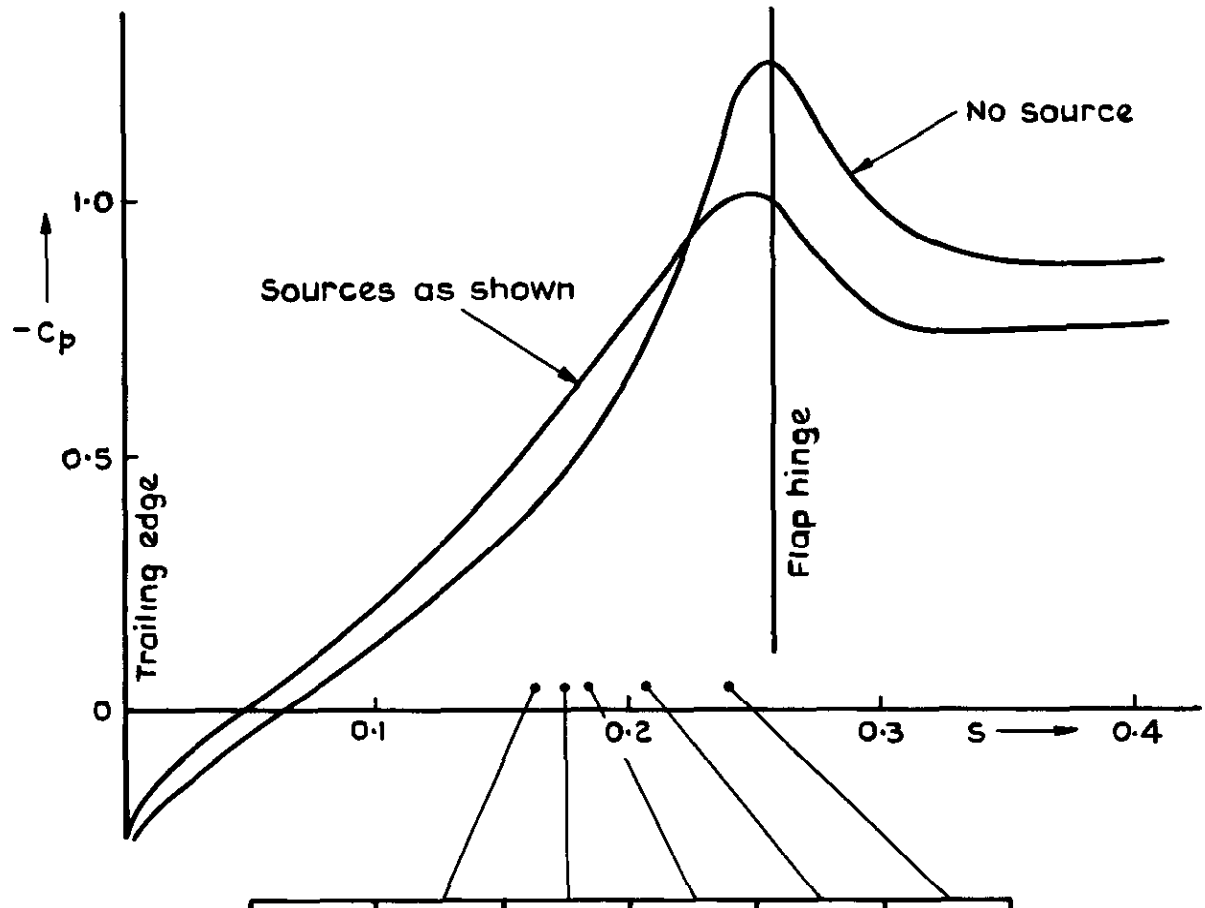

h	0·037	0·037	0·037	0·037	0·037
R	1·2	1·2	1·2	1·2	1·2
θ	40·5°	42°	43·5°	46·5°	51°
m	0·00005	0·0003	0·0012	0·0042	0·0136

Profile P(1·0, 0·25, 0·1, 0·1) (flap angle 18°)

Far flow $U_0 = 1·0$ angle of attack = 0·05 π rad ($\simeq 9°$)

	No source	Sources as shown
Lift coefficient	2·25	2·17
Max flap adverse pressure gradient	15·58	6·16

$U_0 C_F = 0·019$ $C_{LQ} = 0·5$

Fig. 11 Second comparison case pressure curves
Second solution — systematic

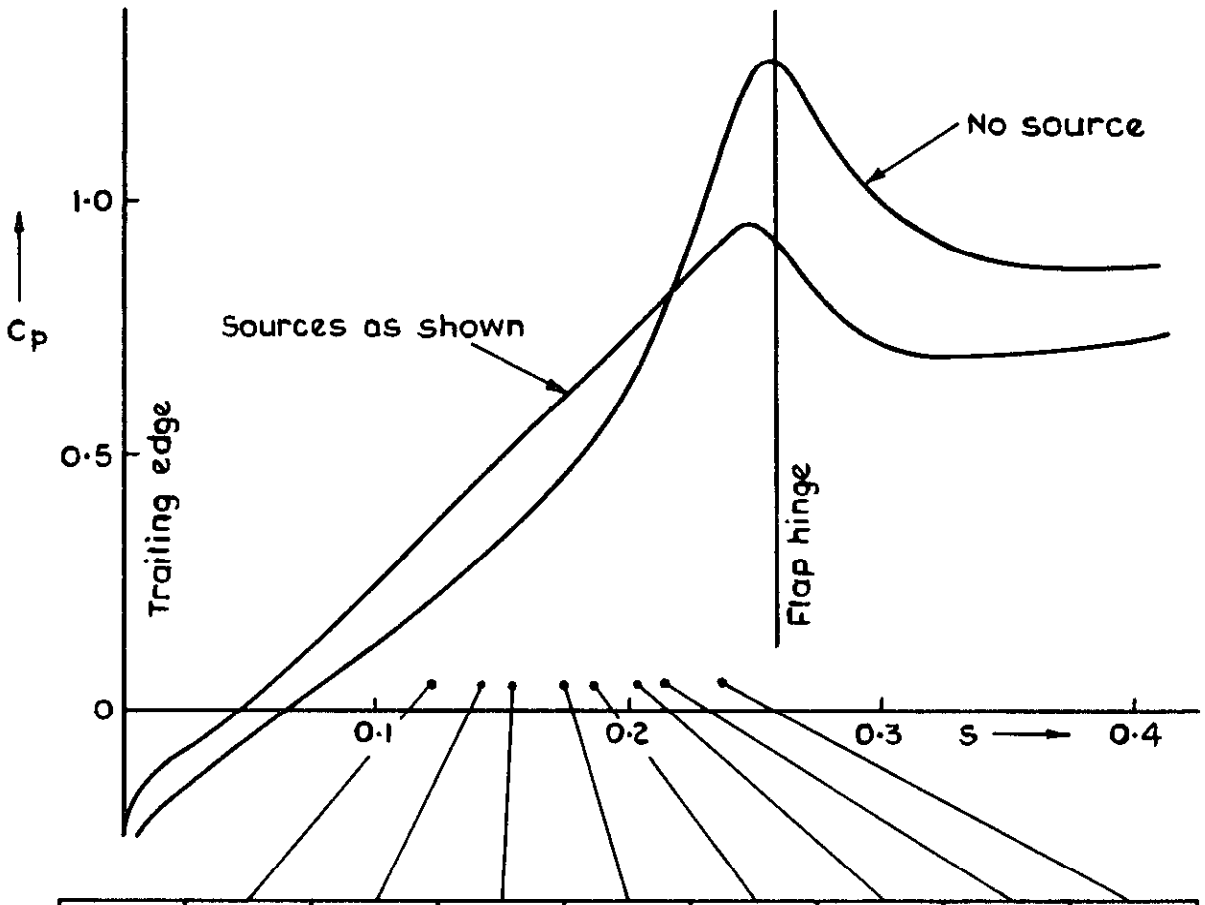

h	0·033	0·035	0·036	0·037	0·037	0·037	0·037	0·037
R	1·2	1·2	1·2	1·2	1·2	1·2	1·2	1·2
θ	34·5°	37·5°	39°	42°	43·5°	46·5°	48°	51°
m	0·00012	0·0012	0·0001	0·0031	0·0003	0·0058	0·00004	0·015

Profile P (1·0, 0·25, 0·1, 0·1) (flap angle 18°)

For flow $U_o = 1·0$, angle of attack = $0·05\pi$ rad ($\simeq 9°$)

	No source	Sources as shown
Lift coefficient	2·25	2·14
Max flap adverse pressure gradient	15·58	5·0

$U_o C_F = 0·032$ $C_{LQ} = 0·47$

Fig. 12 Second comparison case pressure curves
Third solution — systematic

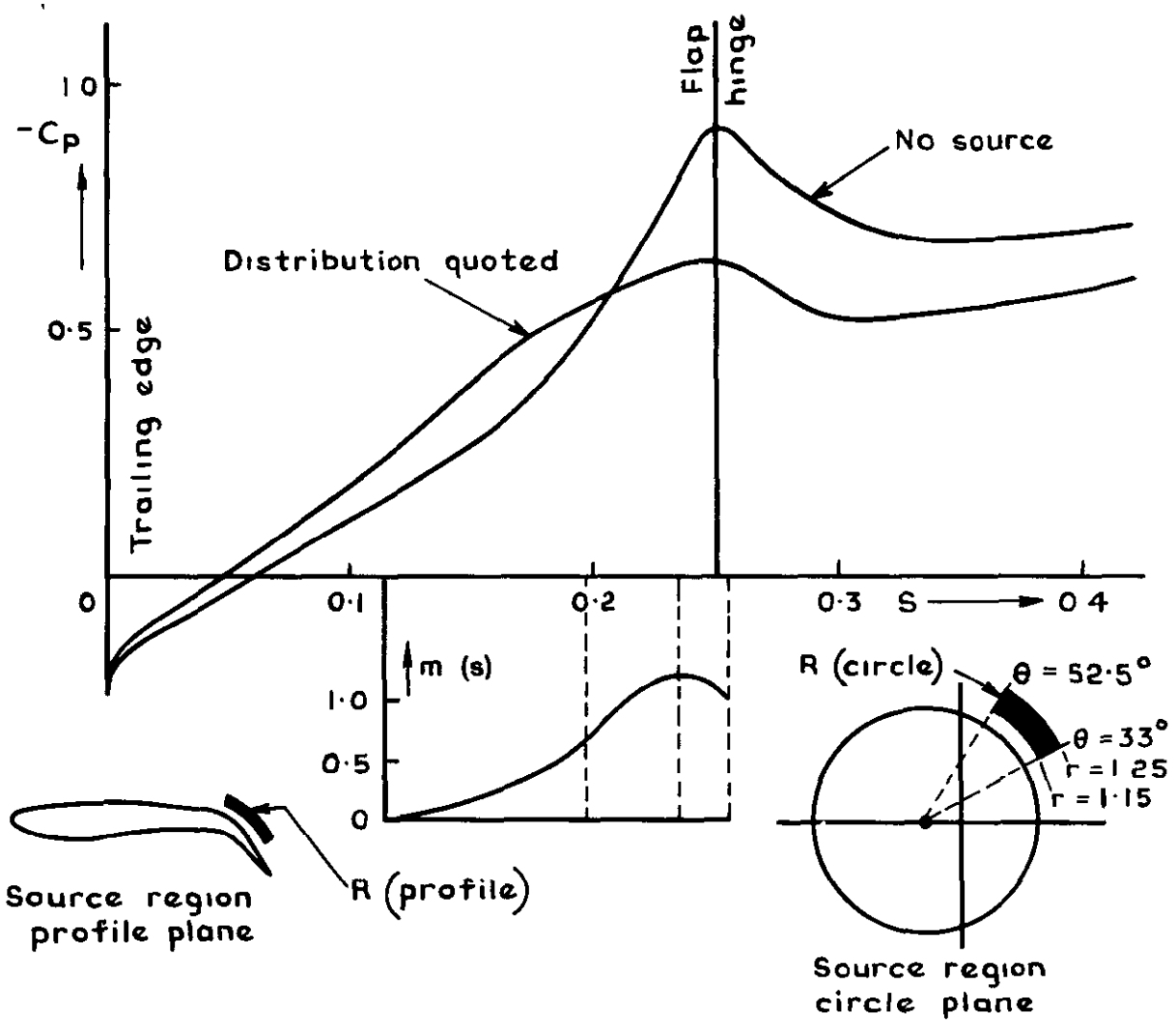

The detailed source distribution is given in section 4·5

Profile P (1·0, 0 05, 0·075, 0·1) (flap angle 13 5°)

Far flow $U_o = 1·0$, angle of attack = 0 05 π rad ($\simeq 9°$)

	No source	Distribution quoted
Lift coefficient	1·96	1 88
Max flap adverse pressure gradient	10·34	4·19

$U_o C_F = 0\ 032$ $C_{LQ} = 0\ 21$

Fig. 13 First comparison case pressure curves continuous source distribution

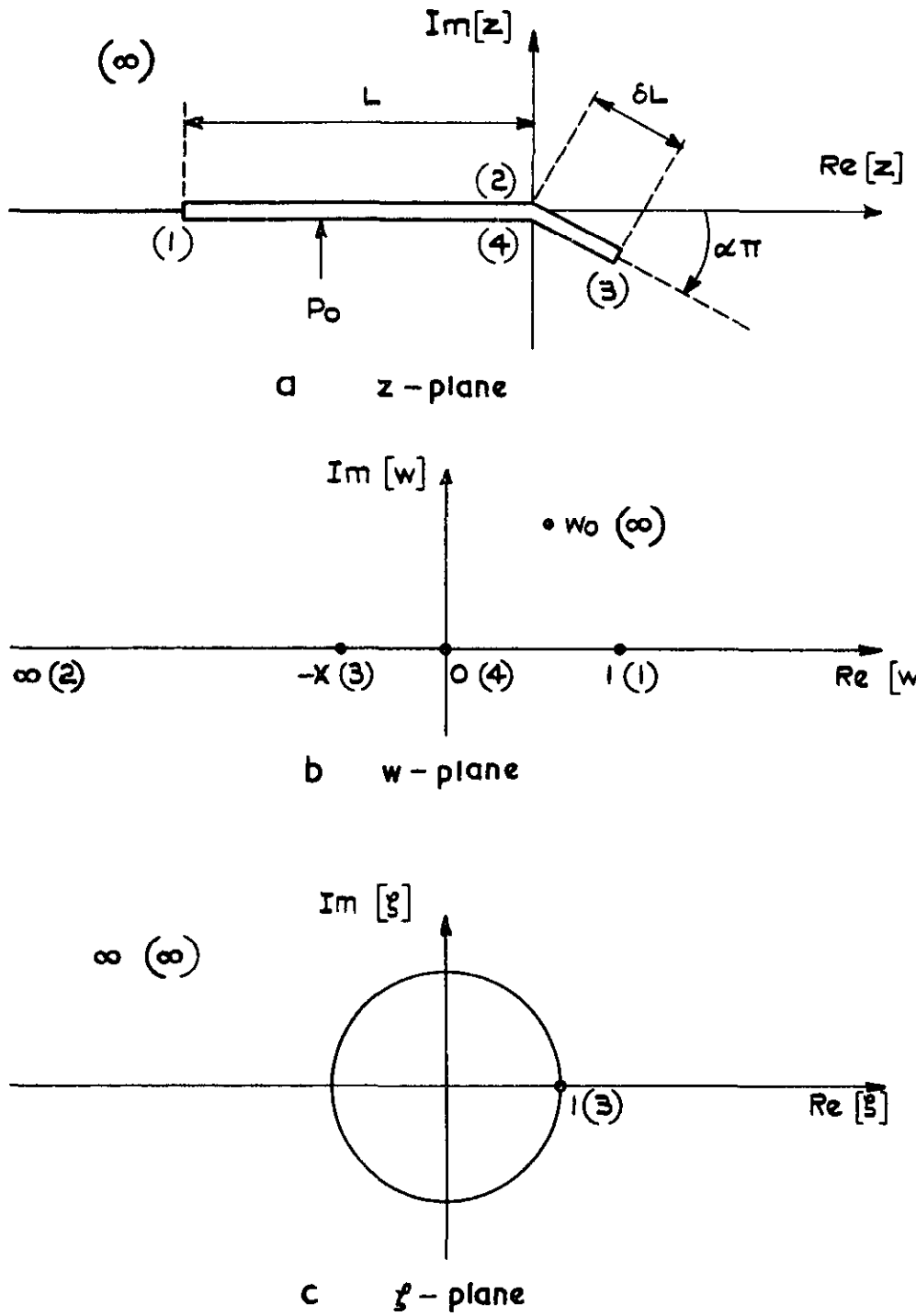

Symbols in brackets refer to points in the first figure

Fig 14 a–c Stages in constructing a flapped aerofoil: mapping skeleton onto unit circle

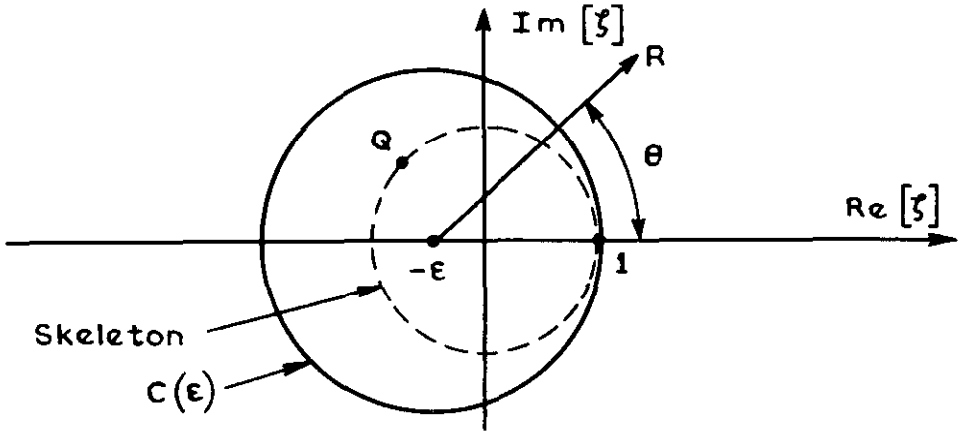

a ζ – plane

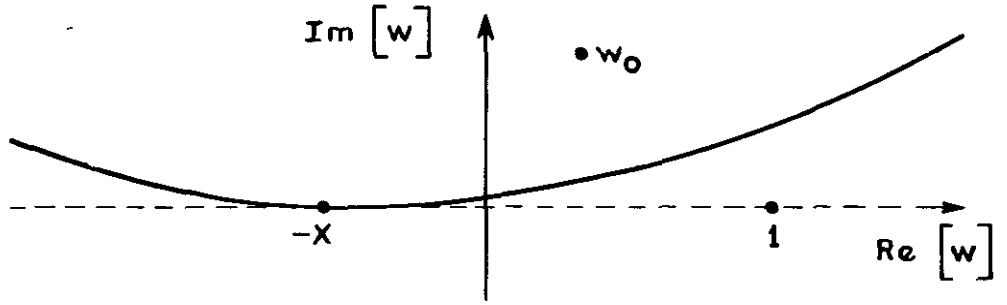

b w – plane

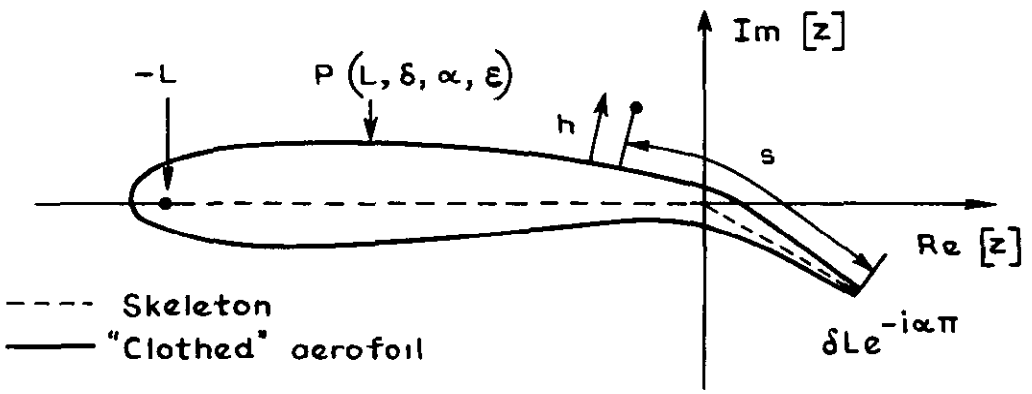

c z – plane

ζ	w	z
∞	w_0	∞
1	-X	$\delta L e^{-i\alpha\pi}$
Q	1	-L

d Correspondence of points under f & g

Fig. 15a-d Stages in constructing a flapped aerofoil: mapping of "clothed" circle onto aerofoil

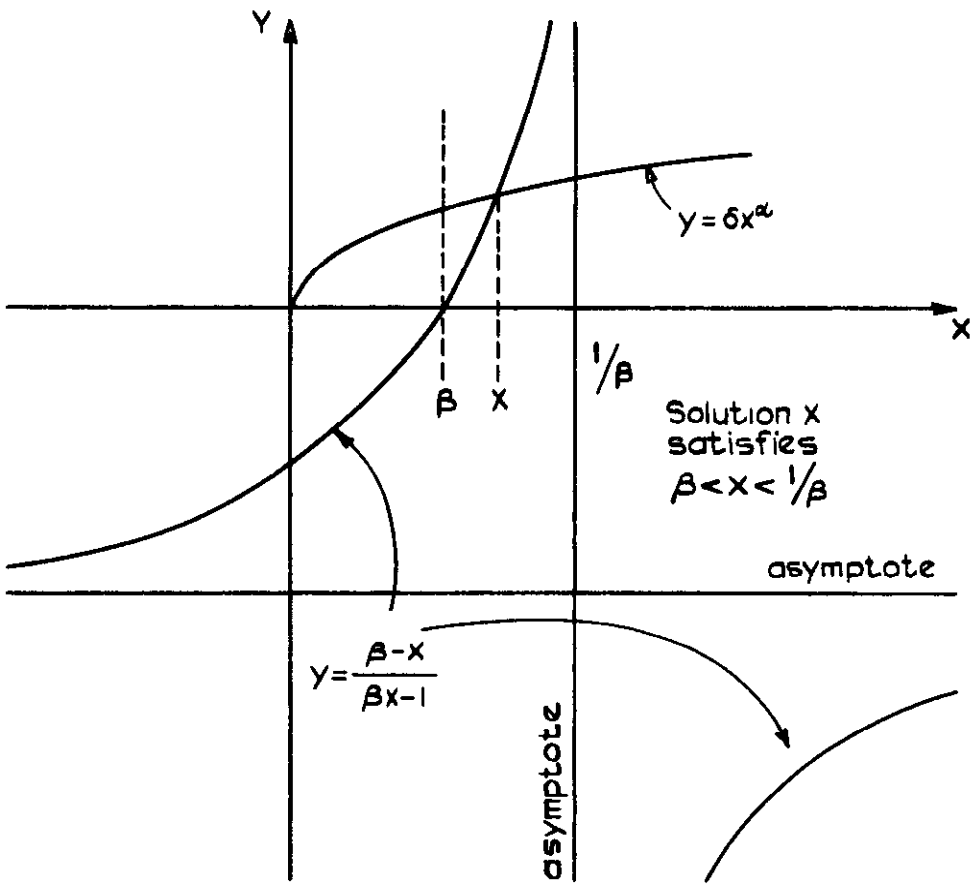

Fig.16 Graphical solution of $\delta = x^{-\alpha}(\beta - x)/(\beta x - 1)$
for $0 < \alpha < 1$ and $0 < \beta < 1$

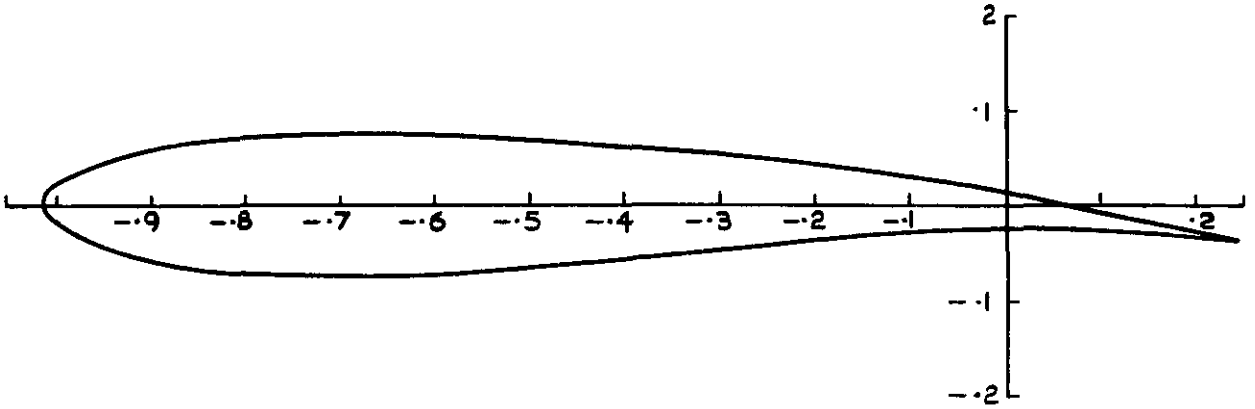

a $\alpha = 0{\cdot}05,\ \delta = 0{\cdot}25,\ L = 1,\ \epsilon = 0{\cdot}1$
(flap angle 9°)

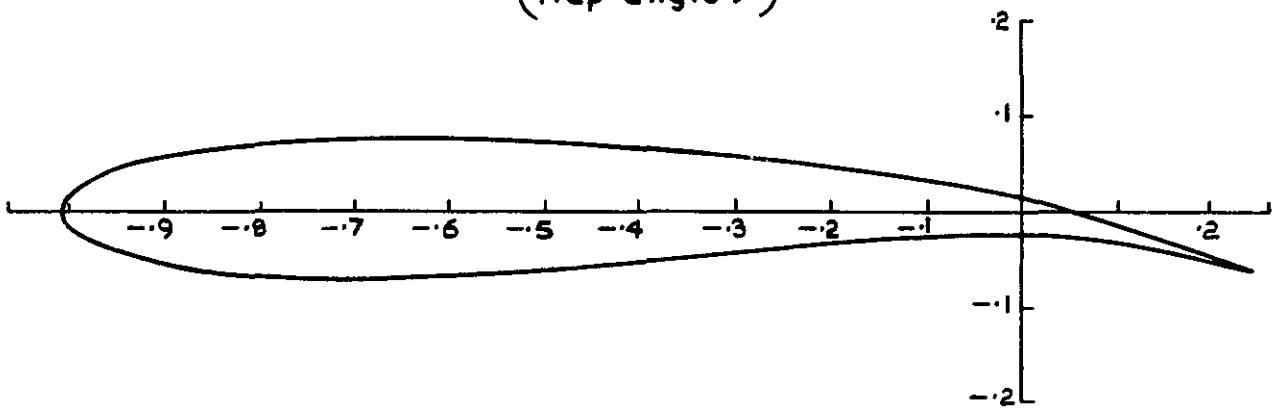

b $\alpha = 0{\cdot}075,\ \delta = 0{\cdot}25,\ L = 1,\ \epsilon = 0{\cdot}1$
(flap angle 13·5°)

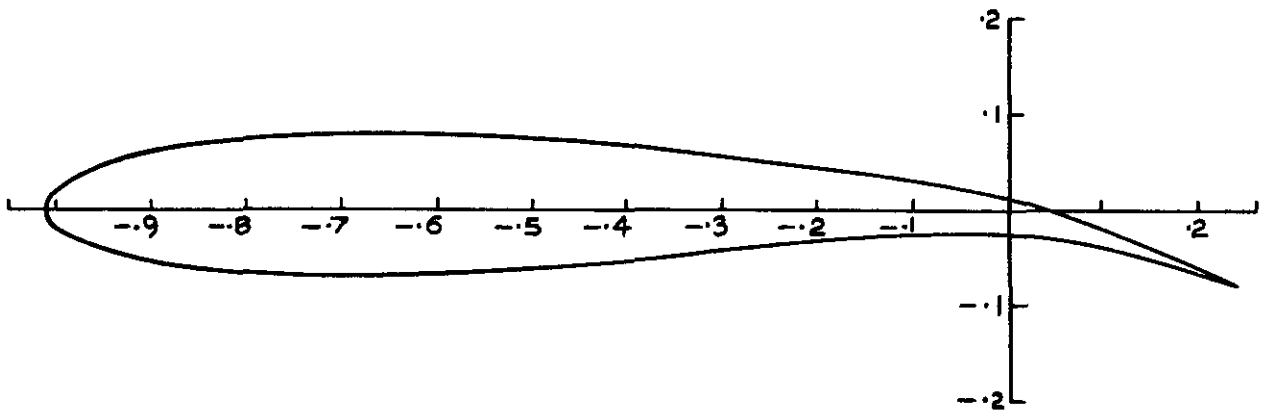

c $\alpha = 0{\cdot}1,\ \delta = 0{\cdot}25,\ L = 1,\ \epsilon = 0{\cdot}1$
(flap angle 18°)

Fig.17a–c Aerofoil under various conditions of flap constructed by method of appendix A

Printed in England for Her Majesty's Stationery Office by the Royal Aircraft Establishment Farnborough Dd 505716 K4 5/73

ARC CP No 1252
January 1972

533 694 65
533 694 511
533 6 048 2
533 694 7

Martin, J

A SUGGESTION FOR IMPROVING FLAP EFFECTIVENESS BY HEAT ADDITION

The effect of a particular type of heat addition on the flow around a twodimensional, flapped aerofoil section, at low Mach number, is investigated using a transformation which enables the compressible flow with heat addition to be deduced approximately from a certain incompressible flow with fluid addition The incompressible flow may be determined by the technique of conformal mapping. It is concluded that heat addition in a suitable distribution can so reduce the adverse pressure gradient on the upper surface of the flap that greater flap angles than are normally possible can be employed without separation of the boundary layer (according to a simple separation criterion) The result is an increase in lift The effect is illustrated for a flapped aerofoil section of convenient mathematical form.

These abstract cards are inserted in Technical Reports for the convenience of Librarians and others who need to maintain an Information Index

Cut here

ARC CP No 1252
January 1972

533 694 65
533 694 511
533 6 048 2
533 694 7

Martin, J

A SUGGESTION FOR IMPROVING FLAP EFFECTIVENESS BY HEAT ADDITION

The effect of a particular type of heat addition on the flow around a twodimensional, flapped aerofoil section, at low Mach number, is investigated using a transformation which enables the compressible flow with heat addition to be deduced approximately from a certain incompressible flow with fluid addition The incompressible flow may be determined by the technique of conformal mapping It is concluded that heat addition in a suitable distribution can so reduce the adverse pressure gradient on the upper surface of the flap that greater flap angles than are normally possible can be employed without separation of the boundary layer (according to a simple separation criterion) The result is an increase in lift The effect is illustrated for a flapped aerofoil section of convenient mathematical form

Cut here

DETACHABLE ABSTRACT CARDS

ARC CP No 1252
January 1972

533 694 65
533 694 511
533 6 048 2
533 694 7

Martin, J

A SUGGESTION FOR IMPROVING FLAP EFFECTIVENESS BY HEAT ADDITION

The effect of a particular type of heat addition on the flow around a twodimensional, flapped aerofoil section, at low Mach number, is investigated using a transformation which enables the compressible flow with heat addition to be deduced approximately from a certain incompressible flow with fluid addition The incompressible flow may be determined by the technique of conformal mapping It is concluded that heat addition in a suitable distribution can so reduce the adverse pressure gradient on the upper surface of the flap that greater flap angles than are normally possible can be employed without separation of the boundary layer (according to a simple separation criterion) The result is an increase in lift The effect is illustrated for a flapped aerofoil section of convenient mathematical form

Cut here

DETACHABLE ABSTRACT CARDS

1973

Published by
HER MAJESTY'S STATIONERY OFFICE

To be purchased from
49 High Holborn, London WC1 V 6HB
13a Castle Street, Edinburgh EH2 3AR
109 St Mary Street, Cardiff CF1 1JW
Brazennose Street, Manchester M60 8AS
50 Fairfax Street, Bristol BS1 3DE
258 Broad Street, Birmingham B1 2HE
80 Chichester Street, Belfast BT1 4JY
or through booksellers

C.P. No. 1252

SBN 11 470810 X